AEDC-TR-70-273

cy 2

PREDICTION OF MOLECULAR SCATTERING EFFECTS IN FREE-JET EXPANSIONS

J. A. Benek

ARO, Inc.

January 1971

VON KÁRMÁN GAS DYNAMICS FACILITY
ARNOLD ENGINEERING DEVELOPMENT CENTER
AIR FORCE SYSTEMS COMMAND
ARNOLD AIR FORCE STATION, TENNESSEE

NOTICES

When U. S. Government drawings specifications, or other data are used for any purpose other than a definitely related Government procurement operation, the Government thereby incurs no responsibility nor any obligation whatsoever, and the fact that the Government may have formulated, furnished, or in any way supplied the said drawings, specifications, or other data, is not to be regarded by implication or otherwise, or in any manner licensing the holder or any other person or corporation, or conveying any rights or permission to manufacture, use, or sell any patented invention that may in any way be related thereto.

Qualified users may obtain copies of this report from the Defense Documentation Center.

References to named commercial products in this report are not to be considered in any sense as an endorsement of the product by the United States Air Force or the Government.

PREDICTION OF MOLECULAR SCATTERING EFFECTS IN FREE-JET EXPANSIONS

J. A. Benek
ARO, Inc.

FOREWORD

The work reported herein was jointly sponsored by Headquarters, Arnold Engineering Development Center (AEDC), Air Force Systems Command (AFSC), Arnold Air Force Station, Tennessee, under Program Element 65701F, Project 4344 and AFCRL, L. G. Hanscom Field, Bedford, Massachusetts, under Program Element 62101F.

The results of the research were obtained by ARO, Inc. (a subsidiary of Sverdrup & Parcel and Associates, Inc.), contract operator of AEDC, AFSC, under Contract F40600-71-C-0002. The work was performed under ARO Project Nos. SW5009 and SW3001 during the period from April to May 1970. The manuscript was submitted for publication on September 21, 1970.

The author expresses his thanks to Messrs. R. F. Brown, J. H. Heald, and M. R. Busby of ARO, Inc., and T. R. Grovers of the University of Toronto for their cooperation in providing either unpublished data or additional information regarding data currently in print. The author acknowledges Mr. W. B. Stephenson of ARO, Inc., for many enlightening discussions in the course of development of the model.

This technical report has been reviewed and is approved.

Eules L. Hively
Research and Development
Division
Directorate of Technology

Harry L. Maynard
Colonel, USAF
Director of Technology

ABSTRACT

The effects of background pressure on reduction of molecular beam intensity are investigated. A theoretical model is developed which shows the background to be separable into two distinct components: one attributable to reflected jet particles and the other attributable to residual (unpumped) particles. An expression for the Fenn and Anderson correlation parameter is obtained. Comparisons of the data of several investigators are made with theoretically predicted values of intensity as a function of either separation distance or source pressure. The characteristic dip in the intensity versus source pressure curve has been related to scattering effects as well as to condensation effects.

CONTENTS

APPENDIXES

Figure | Page

NOMENCLATURE

A_{SK}	Skimmer orifice area
C	Magnitude of the total random molecular velocity vector of scattering particles
C_B	Mean molecular velocity based on reflected gas temperature
C_b	Mean molecular velocity based on random background temperature
C_s	General scattering particle mean molecular velocity
D	Source orifice diameter
D_d	Detector orifice diameter
d	Skimmer height
F	Fraction of particles readmitted by wall
f	Molecular flux at freezing surface
g_{AB}	Relative collision velocity
g_{js}	Relative jet-scattering particle collision velocity
I	Intensity (measured)
I_o	Reference $1/X^2$ varying intensity
I*	Ideal measured intensity dependent on system geometry

Kn_N	Knudsen number based on source conditions and diameter
k	Boltzmann constant
ℓ_s	Classical theory scattering length
M_{fs}	Mach number at freezing surface
n^*	Sonic number density
n_B	Background number density based on reflected jet particles
n_{b_∞}	Background number density based on residual gas particles
n_j	Number density of jet
n_{jw}	Number density of jet evaluated at the wall radius r_w
n_s	General scattering number density
P_B	Reflected background component of pressure
P_{b_∞}	Disturbed residual gas background pressure
P_o	Source pressure
P_s	General scattering particle pressure
r	Source-skimmer separation distance
r^*	Sonic radius
r_d	Skimmer orifice-detector separation distance
r_{fs}	Radius of freezing surface
r_s	Freezing surface-skimmer separation distance
r_{SK}	Radius of skimmer orifice
r_w	Source-wall separation distance
r'_w	Distance from the origin to any point on the wall
T^*	Sonic temperature
T_B	Temperature of reflected background

T_b	Temperature of residual background
T_s	General scattering particle temperature
V_j	Free-stream velocity of the jet
x	Dummy separation variable
Z_{AB}	Collision frequency between species A and Species B
Z_{js}	Jet-scattering particle collision frequency
Z_{sj}	Scattering particle-jet collision frequency
γ	Ration of specific heats
δ	Parameter expressing amount of change in molecular velocity per collision
ϵ	Collision parameter (See Fig. 4)
ζ	Parameter which accounts for the uncertainty in the number of collisions required to effectively stop a background particle
η	Constant resulting from non-dimensionalization of the governing equations
ν	Relative collision velocity
θ	Angle between the centerline and r_w
σ_s	Classical scattering law collision cross section
σ_{BJ}	Background-jet collision cross section (Ref. 8)
σ_{Bj}	Reflected background-jet collision cross section
σ_{bj}	Residual background-jet collision cross section
σ_{JB}	Jet-background collision cross section (Ref. 8)
σ_{jB}	Jet-reflected background collision cross section
σ_{jb}	Jet-residual background collision cross section
ψ	Collision parameter (See Fig. 4)

Note: Bars indicate non-dimensionalized quantities as per Section 2.3.

SECTION I
INTRODUCTION

1.1 GENERAL

Currently, there is extensive interest in investigation of the rarefied portions of highly expanded rocket exhaust plumes. In particular, parameters such as condensation, species concentrations, and species velocity distributions are of fundamental importance. The molecular beam technology has been demonstrated to be exceptionally well suited to the measurement of these parameters. Studies made in molecular beam chambers and in the development of a mass-spectrometer sampling probe indicate that molecular scattering phenomena are a dominant factor in beam system design and data interpretation (Ref. 1). Hence, the desirability of establishing a theoretical model which may be employed to predict the magnitude of molecular scattering effects has become clearly evident.

1.2 BACKGROUND

The first high intensity molecular beam work was based on the principle postulated by Ashkenas and Sherman (Ref. 2) that the background had no effect on the portion of the flow field contained within the barrel shock structure. This conclusion was deduced from extensive theoretical studies using the method of characteristics to determine various flow field properties. As a result of this premise, they made additional studies to determine the location of the Mach disc, and hence, to define the maximum axial distance of undisturbed flow. These investigations led to an empirical expression for Mach disc position (Ref. 2).

The problem of background interaction with rarefied jet expansion was first considered in depth by Fenn and Anderson (Ref. 3). They reasoned that such interaction could result when the shock structure became diffuse during extreme rarefaction. Their study showed that such an interaction did, in fact, exist and is characterized by scattering of the jet by the background gas. They concluded that the jet becomes porous to the background, and at sufficiently large nozzle-skimmer separations, the background concentration is the same inside and outside the jet. They also concluded that a critical distance from the source exists such that, at separations less than this value, the background is quickly attenuated leaving a region of undisturbed jet. Fenn and Anderson developed an empirical parameter from the classical scattering law to characterize the degree of interaction. They correlated their data as well as that of other investigators for beam attenuation using this parameter.

A subsequent investigation by Brown and Heald (Ref. 4) using a cryogenically pumped test volume yielded data which are in poor agreement with the trends of Ref. 3. While some of this variation may be attributable to the test conditions, a recent study made by Benek and Powell (Ref. 1) indicates that some of this difference can be traced to the difference in the location of the background pressure measurement (Fig. 1, Appendix I). This implies that there is a variety of difficulties in the experimental determination of background effects.

Bossel (Ref. 5) conducted an extensive investigation of the dependence of measured jet flux on several parameters. He found that the skimmer-orifice, chamber-wall separation distance had an important effect on the jet flow. These results indicate the importance of wall effects, especially at high flow rates.

A detailed study was conducted by Govers, et al (Ref. 6) who investigated parameters governing the location of the peaks of the intensity separation distance curves (Fig. 2a). Their results indicated that the skimmer geometry was also a factor governing the location of the maxima.

A subsequent investigation into the means to eliminate skimmer flow-field interaction was made by Ruby (Ref. 7). It was found that a cryogenically cooled toroidal skimmer could reduce this interaction to insignificant values. Ruby's findings are discussed in detail in Section 3.3.

Theoretical treatments of the scattering process have only recently appeared in the literature. An informative model has been presented by Muntz, et al (Ref. 8) where an expression is obtained for the correlation parameter suggested by Fenn and Anderson. However, this relation does not agree well with the available data.

Shaw and Hickman (Ref. 9) have considered the penetration of background particles into a simulated rocket exhaust plume. By reasoning quite similar to that employed by Muntz, et al, these investigators were led to an expression for the loss of the jet flux due to interaction with the background gas. The form of this expression agrees with that in Ref. 8.

The present analysis attempts to construct a model of the molecular scattering process which can be used to predict values of molecular flux measured by a given detector geometry under specified source and background conditions. The model and pertinent introductory material are discussed in the next section.

SECTION II
ANALYSIS

2.1 FENN AND ANDERSON CORRELATION PARAMETER

The typical effects of background scattering are illustrated in Fig. 2a. There is an exponential decrease in the measured intensity (i.e. density) with background pressure. This dependence is demonstrated in Fig. 2b which is a semilog cross-plot of the data in Fig. 2a. The linear variation indicates that the classical scattering law

$$\frac{I}{I_o} = \exp\left\{ - n_s \sigma_s^2 \ell_s \right\}$$

applied to a given jet could, in principle, describe the phenomenon. By taking the scattering length (ℓ_s) and cross-section (σ_s^2) and the unscattered intensity (I_o) to be

constant, and employing the perfect gas equation of state per molecule, the linear dependence on background pressure becomes,

$$\ell n \frac{I}{I_o} = - P_s \left(\frac{\sigma_s^2 \ell_s}{k T_s} \right) = - P_s \text{ (constant)}$$

This reasoning leads to the correlation parameter suggested by Fenn and Anderson (Ref. 3):

$$- \frac{\partial}{\partial P_{b_\infty}} \left(\ell n \frac{I}{I_o} \right) \Bigg|_{\substack{\ell_s = \text{const} \\ \sigma_s^2 = \text{const}}} = \text{[Constant]} \qquad (1)$$

Equation (1) corresponds to the change in measured intensity per unit change of background pressure.

Although not stated explicitly in the arguments leading to Eq. (1), there are several significant properties implied by its form. First, the background pressure does not appear in the correlation parameter. This indicates that any dependence on the magnitude of the background pressure must necessarily be of second order, at most. This point will be important in the discussion in Section IV. Second, a suitable definition for the scattering length (ℓ_s) is required because the flow is continuum or near continuum for several source diameters downstream of the orifice and background particles cannot penetrate this region of the expansion. Third, ℓ_s must be at least an indirect function of the source conditions since they determine the extent of the continuum region of the flow.

2.2 PROPOSED MODEL

An attempt has been made in the present formulation to keep the model of the scattering process as elementary as possible while retaining the essential properties of the phenomenon. In keeping with this philosophy, a spherical source of radius r* producing a spherically symmetric flow field has been chosen to represent the jet (Fig. 3).

The background is assumed to be composed of two independent components. One of these results from scattered jet particles which are reflected back into the jet after collision with the wall. The other background component is a result of gases which are not removed by the pumping system. These components are assumed to be completely random, with a thermal velocity associated with the wall temperature and homogeneous in the absence of the jet. It is assumed that the skimmer (Fig. 1) is of infinitesimal diameter. This corresponds to replacing the skimmer with a flat wall and determining the value of the incident flux at a distance, d, from the wall (Fig. 3). Finally, the interactions of the background-jet and jet-background are assumed to be independent of each other.

The general procedure to be followed is to calculate a background distribution in the absence of the jet expansion. This ideal background is then altered by collisions with an undisturbed jet and then the jet is scattered by interaction with the resultant background distribution.

2.3 GOVERNING EQUATIONS AND DISCUSSION

2.3.1 The Mathematical System

The system of governing equations for the general model discussed in Section 2.2 is obtained from the following considerations: First, the source is assumed to be spherical with angular symmetry. Second, the density variation along a streamline is determined by the appropriate collision frequency, as defined in Section 2.4. Thus, consideration of continuity must include a "sink" or depletion term proportional to the collision frequency to account for the density change. This leads to

$$C_s \frac{dn_s}{dx} = Z_{sj} \tag{2}$$

$$V_j \frac{d(x^2 n_j)}{x^2 dx} = -Z_{js} \tag{3}$$

where

C_s = general scattering particle mean molecular velocity

V_j = free-stream velocity of the jet

n_s = number density of scattering particles

n_j = number density of jet

Z_{sj} = scattering particle-jet collision frequency

Z_{js} = jet-scattering particle collision frequency

x = dummy separation variable

The form of Eq. (2) results from an attempt to describe the randomness of the background; i.e., it has no perferred direction and in the absence of the jet gives a uniform distribution of the scattering number density (n_s). Equation (3) results from the spherical geometry and, in the absence of scattering, gives the usual $1/x^2$ dependence of n_j generally associated with the expansion process.

2.3.2 The Nondimensional System

A set of nondimensional variables signified by the bars are defined according to

$$\bar{n}_j = \frac{n_j}{n^*}, \quad \bar{n}_s = \frac{n_s}{n^*}, \quad \bar{C}_s = \frac{C_s}{V_j}, \quad \bar{\nu} = \frac{\nu}{V_j}$$

$$\bar{\sigma}_{sj}^2 = \frac{\sigma_{sj}^2}{D^2}, \quad \bar{\sigma}_{js}^2 = \frac{\sigma_{js}^2}{D^2}, \quad \eta = n^* D^3$$

$$\bar{x} = \frac{x}{D}, \quad \bar{Z}_{sj} = \frac{Z_{sj}}{n^{*2} D^2 V_j}, \quad \bar{Z}_{js} = \frac{Z_{js}}{n^{*2} D^2 V_j}$$

where n^* is the sonic density, D is the source orifice diameter, and V_j is the aerodynamic streaming velocity. Equations (2) and (3) can then be written in nondimensional form as

$$\bar{C}_s \frac{d\bar{n}_s}{d\bar{x}} = \eta \bar{Z}_{sj}$$

$$\frac{d(\bar{x}^2 \bar{n}_j)}{\bar{x}^2 d\bar{x}} = \eta \bar{Z}_{js} \tag{4}$$

2.4 COLLISION FREQUENCY TERM

The collision frequency terms required by the previous section were obtained from the kinetic theory. The general expression for the number of collisions per unit time per unit volume per particle between the hard sphere species A and B (Z_{AB}) is given by

$$Z_{AB} = \int_{V_x} \int_{V_z} \int_{\epsilon} \int_{\psi} n_A n_B \sigma_{AB}^2 f_A(Z_j) f_B(C_j) g_{AB} \sin\psi \cos\psi \, d\psi \, d\epsilon \, dV_z \, dV_c$$

where n_A, n_B = respective number densities of species A and B

f_A, f_B = respective velocity distributions

g_{AB} = relative collision velocity

ψ, ϵ = collision parameters defined in Fig. 4

σ_{AB}^2 = collision cross section

dV_c, dV_z = respective volume elements in velocity space

Because of the narrow distribution of velocities associated with an aerodynamically accelerated flow (Ref. 10), the distribution function f_A for the jet molecules may be approximated by an impulse function, i.e. $f_A = 1$ for velocities within dV_z of V_j, and $f_A = 0$ for velocities outside this range. Here V_j is the aerodynamic streaming velocity of the jet.

The relative collision velocity between jet and background particles (g_{js}) is defined as

$$g_{js} = [(C_1 - V_j)^2 + C_2^2 + C_3^2]^{1/2}$$

or

$$g_{js} = [C^2 + 2C_1 V_j + V_j^2]^{1/2}$$

where

$$C^2 = C_1^2 + C_2^2 + C_3^2$$

and C is the magnitude of the random thermal velocity vector of the background particles.

Since V_j is larger than the random velocity (C) and since the components of C are assumed to be of the same order as C_1 the approximation

$$g_{js} = (C + V_j) \tag{6}$$

is permitted.

By assuming that the scattering particles are described by a Maxwellian distribution (f_B), substitution of the approximation for f_A, f_B, and Eq. (6) into Eq. (5) and transformation into spherical coordinates in velocity space give

$$Z_{js} = \int_{\epsilon} \int_{\psi} \int_{V_c} 4\pi n_j n_s \sigma_{js}^2 \left(\frac{m_s}{2kT_s}\right)^{3/2} (C + V_j)\, C^2 \exp\left(-\frac{m_s}{2kT_s} C^2\right) dV_c \sin\psi \cos\psi\, d\psi\, d\epsilon \tag{7}$$

Integration of Eq. (7) over the ranges,

$$C = 0 \text{ to } \infty,\ \epsilon = 0 \text{ to } 2\pi, \text{ and } \psi = 0 \text{ to } \pi/2$$

yields

$$Z_{js} = n_j n_s \left[\left(\frac{2\,k\,T_s}{m_s}\right)^{1/2} \frac{2}{\pi^{1/2}} + V_j\right] \sigma_{js}^2$$

The first term in the brackets is recognized to be the mean speed $\langle C_s \rangle$ which defines

$$\nu_{js} = \langle C_s \rangle + V_j \tag{8}$$

where $\langle C_s \rangle$ is the mean speed of scattering particles and V_j is approximately the mean speed of the jet particles. The approximate result for the jet-scattering particle collision frequency is

$$Z_{js} = n_j n_s \sigma_{js}^2 \nu_{js} \tag{9a}$$

Similarly, an expresssion for the scattering particle-jet collision frequency can be obtained, i.e.,

$$Z_{sj} = n_s n_j \sigma_{js}^2 \nu_{sj} \tag{9b}$$

Note that

$$\nu_{sj} = \nu_{js} = \nu$$

2.5 WALL SCATTERING EFFECT

The problem presented by gas surface interaction is an extremely complicated one and is far beyond the scope of this work. In order to introduce the gross effects of the chamber walls while avoiding the complex mechanisms of the process, the following model is adopted: An infinite wall at a distance $\bar{r}_w$ from a spherical source of radius $\bar{r}^*$ captures incident molecules. After capture, the molecules are accommodated to the wall temperature, and a fraction (F) is readmitted into the incident jet with a thermal velocity $\bar{C}_B$ corresponding to the wall temperature. The subscript B will be used to designate the wall scattering component of the background. The model and associated coordinate system are shown in Fig. 3.

By following the procedure outlined in Section 2.2, the undisturbed spacial distribution of reflected jet particles can be calculated if it is assumed that no collisions occur between the jet and background. As a first approximation, the wall in Fig. 3 was assumed to consist of a distribution of point sources. The strength of each source was assumed to be proportional to the incident number density at that point. The incident number density was determined from the relation quoted by French (Ref. 11) for the off-axis density in a free-jet expansion. This can be written in the form

$$\bar{n}_j (r_w', \theta) = \frac{A}{\bar{r}_w'^2} \cos^2 (B\theta)$$

where $\bar{r}_w'$ is the distance from the origin of the spherical source to any point on the wall, θ is the angle between the centerline and $\bar{r}_w'$, and A and B are constants depending on the source conditions. In practice, B lies close to 1.0, and for the first approximation, the value B = 1.0 was used. The constant A was taken to be $A = [(\gamma + 1)/2]/\bar{r}^{*2}$ where γ is the ratio of specific heats in the source.

The number density incident on an element of area is found to be proportional to $\cos^3\theta$. This causes the distribution on the wall to be narrow with the maximum near the centerline and a rapid decrease away from it. This indicates that a further approximation might be made by assuming that a point source lies on the surface at the centerline with a strength such that the number density at the wall is

$$\bar{n}_{B_w} \equiv F\bar{n}_{jw} = F\left(\frac{\bar{r}^*}{\bar{r}_w}\right)^2 \tag{10}$$

where F is the fraction of incident molecules that are readmitted by the surface and $\bar{n}_{jw}$ is the undisturbed number density evaluated at the wall. However, a source located on the surface of the wall introduces a singularity at $x = \bar{r}_w$ such that

$$\lim_{\bar{x} \to \bar{r}_w} \bar{n}_B \to \infty$$

To avoid this problem and satisfy the condition on the wall given by Eq. 10, it is convenient to assume that the background varies as

$$\bar{n}_B = \frac{\bar{n}_{B_w}}{(1 + \bar{r}_w - \bar{x})^2} = \frac{F\,\bar{n}_{jw}}{(1 + \bar{r}_w - \bar{x})^2} \tag{11}$$

which corresponds to locating the background source one jet source diameter behind the wall. Hence Eq. 11 will be adopted as an additional approximation.[1]

The background spacial distribution resulting from the interaction with the undisturbed jet is given by

$$\bar{C}_B \frac{d\bar{n}_B}{d\bar{x}} = \eta \bar{n}_B \bar{n}_j \bar{\sigma}_{Bj}^2 \bar{\nu} \tag{12}$$

Substituting Eq. (11) into Eq. (12), replacing n_j by $(\bar{r}^*/\bar{x})^2$, and integrating subject to the boundary condition (Eq. 10) yield

$$\begin{aligned}\bar{n}_B = {} & F \bar{n}_{jw} \left\{1 + \bar{r}_B \left[\frac{1-\bar{r}_w}{(1+\bar{r}_w)^2 \bar{r}_w} - \frac{2}{(1+\bar{r}_w)^2} \ell n \bar{r}_w\right]\right\} \\ & - F \bar{n}_{jw} \bar{r}_B \left\{\frac{1+\bar{r}_w-2\bar{x}}{(1+\bar{r}_w)^2 \bar{x} (1+\bar{r}_w-\bar{x})}\right. \\ & \left. + \frac{2}{(1+\bar{r}_w)^3} \ell n \left(\frac{1-\bar{r}_w-\bar{x}}{\bar{x}}\right)\right\}\end{aligned} \tag{13}$$

where

$$\bar{r}_B \equiv \frac{\bar{\nu} \bar{\sigma}_{Bj}^2 \bar{r}^{*2} \bar{\eta}}{\bar{C}_B}$$

The loss of molecules from the jet is governed by

$$\frac{d(\bar{x}^2 \bar{n}_j)}{\bar{x}^2 d\bar{x}} = - \eta \bar{n}_j \bar{n}_B \bar{\sigma}_{jB}^2 \bar{\nu} \tag{14}$$

Substituting Eq. (13) into Eq. (14) and integrating from $\bar{r}^*$ to $\bar{r}$ give

$$\begin{aligned}\ell n \frac{I}{I_o}\bigg|_w = {} & -\Gamma_B \bar{n}_{jw} F \left\{1 + \bar{r}_B \left[\frac{1-\bar{r}_w}{(1+\bar{r}_w)^2 \bar{r}_w} - \frac{2}{(1+\bar{r}_w)^3} \ell n \bar{r}_w\right]\right\} (\bar{r} - \bar{r}^*) \\ & + \Gamma_B \bar{r}_B \bar{n}_{jw} F \left\{\frac{1}{(1+\bar{r}_w)^2} \left[\ell n \left(\frac{1+\bar{r}_w-\bar{r}}{(1+\bar{r}_w+\bar{r}^*)}\right) + \ell n \left(\frac{\bar{r}}{\bar{r}^*}\right)\right]\right.\end{aligned}$$

[1] As a check of this assumption, the procedure outlined in the remainder of this section was followed using the $\cos^3\theta$ wall distribution rather than Eq. 11. The procedure resulted in a system of integrals which had to be evaluated numerically. A detailed consideration of this system indicated that the form obtained in Eq. 16 accurately describes the effect of the reflected particles on the jet. Therefore, the simplification represented by Eq. 11 is deemed justified.

$$+ \frac{2}{(1+\bar{r}_w)^3}\left[(1+\bar{r}_w-\bar{r})(\ell n\,(1+\bar{r}_w-\bar{r})-1)+\bar{r}(\ell n\,\bar{r}-1)\right]$$

$$-\frac{2}{(1+\bar{r}_w)^3}\left[(1+\bar{r}_w-\bar{r}^*)(\ell n(1+\bar{r}_w-\bar{r}^*)-1)+\bar{r}^*(\ell n\,\bar{r}^*-1)\right]\Bigg\} \qquad (15)$$

where

$$\Gamma_B \equiv \bar{\nu}\bar{\sigma}_{jB}^2\eta, \quad \left.\frac{I}{I_o}\right|_w = \bar{n}_j\left(\frac{\bar{x}}{\bar{r}^*}\right)^2$$

Evaluation of Eq. (15) shows that only the first term in brackets significantly affects the value of $\ell n\, I/I_o|_w$. This may be seen by noting that

$$\bar{n}_{jw} \propto \frac{1}{\bar{r}_w^2}, \quad \bar{r}_w > \bar{r} = \bar{d} + \bar{r}$$

where $\bar{d}$ is generally 50 or greater and all but the first term varies as $\bar{r}_w^{-4}$. Thus Eq. (15) can be approximated by

$$\ell n\left.\frac{I}{I_o}\right|_w = -\Gamma_B F\,\bar{n}_{jw} \qquad (16)$$

Equation (16) represents the loss of jet molecules due to the reflection of molecules from the chamber walls.

2.6 RESIDUAL GAS EFFECT

The residual (i.e., unpumped) gas in the test volume is considered to be completely random and homogeneous in the absence of the jet. The interaction between this background component, which will be designated by the subscript b, and the jet is modeled by placing the spherical source of Section 2.5 in an infinitely large chamber which has a base pressure of $\bar{P}_{b\infty}$ and corresponding number density $\bar{n}_{b\infty}$. The governing equations are of the form of Eq. (4). By following the procedure of Section 2.5, the background distribution in the undisturbed jet is given by

$$\frac{\bar{n}_b}{\bar{n}_{b\infty}} = e^{-\bar{r}_b/\bar{x}} \qquad (17)$$

where

$$\bar{r}_b \approx \frac{\bar{\nu}\,\bar{\sigma}_{bj}\,\bar{r}^{*2}\,\eta}{\bar{C}_b}$$

The loss of molecules from the jet due to collisions with the residual background is then

$$\ell n\left.\frac{I}{I_o}\right|_b = -\bar{n}_{b\infty}\,\Gamma_b\int_{\bar{r}^*}^{\bar{r}}\exp\left(-\frac{\bar{r}_b}{\bar{x}}\right)d\bar{x} \qquad (18)$$

where

$$\Gamma_b = \bar{\nu}\ \bar{\sigma}_{jb}^2\ \eta \text{ and } \left.\frac{I}{I_o}\right|_b = \bar{n}_j\left(\frac{\bar{x}}{\bar{r}^*}\right)^2$$

An evaluation of the integral is presented in Appendix II.

2.7 EXPRESSION FOR THE FENN AND ANDERSON CORRELATION PARAMETER

At this point, an expression for the right hand side of the scattering parameter developed in Section 2.1 can be obtained. According to the present approach, Eq. (1) should be determined by the $\bar{P}_{b_\infty}$ component of background. Thus, Fenn and Anderson's parameter is given by

$$-\frac{\partial}{\partial \bar{P}_{b_\infty}}\left(\ell n\ \left.\frac{I}{I_o}\right|_b\right) = \Gamma_b \frac{\partial \bar{n}_{b_\infty}}{\partial \bar{P}_{b_\infty}} \int_{\bar{r}^*}^{\bar{r}} \exp\left(-\frac{\bar{r}_b}{\bar{x}}\right) d\bar{x}$$

By using the equation of state per molecule, the above may be rewritten as

$$-\frac{\partial}{\partial \bar{P}_{b_\infty}}\left(\ell n\ \left.\frac{I}{I_o}\right|_b\right) = \frac{\Gamma_b}{\bar{T}_{b_\infty}} \int_{\bar{r}^*}^{\bar{r}} \exp\left(-\frac{\bar{r}_b}{\bar{x}}\right) d\bar{x} \tag{19}$$

where

$$\bar{T}_{b_\infty} \equiv \frac{T_{b_\infty}}{T^*},\ \bar{n}_{b_\infty} = \bar{P}_{b_\infty}/\bar{T}_{b_\infty}$$

are the residual background temperature normalized to the source sonic temperature and pressure.

2.8 TOTAL SCATTERING LOSS

The total reduction of the jet by the interactions with the wall and the residual components of the background can be expressed as

$$\ell n\ \left.\frac{I}{I_o}\right|_T = \ell n\ \left.\frac{I}{I_o}\right|_w + \ell n\ \left.\frac{I}{I_o}\right|_b$$

or

$$\left.\frac{I}{I_o}\right|_T = \left(\left.\frac{I}{I_o}\right|_w\right)\left(\left.\frac{I}{I_o}\right|_b\right) \tag{20}$$

It is important to realize at this point that Eq. (20) describes the loss as measured from an ideal $(\bar{x})^{-2}$ density variation in the jet. However, it has been observed that with sufficiently low background levels the measured intensity variation with $\bar{r}$ can exceed this limit, and in some cases nearly constant intensities have been measured (e.g. Ref. 4).

Fenn and Anderson realized that this phenomenon could be related to the detection system configuration. They obtained the following expressions, based on the geometry of Fig. 5, for no background losses.

If $\bar{r}_{fs}$ is small compared to skimmer orifice diameter (r_{SK}),

$$\bar{I}^* = \frac{I^*}{f} = A_{SK} \frac{\gamma M_{fs}^2}{2\pi \bar{r}_d^2} \exp\left[-\frac{\gamma M_{fs}^2}{2}\left(\frac{\bar{r}}{\bar{r}_{fs}}\right)^2\left(\frac{\bar{D}_d}{\bar{r}_d}\right)^2\right] \tag{21}$$

where

f = flux at the freezing surface

M_{fs} = Mach number at the freezing surface

$\bar{r}_{fs}$ = distance from source to freezing surface

A_{SK} = skimmer orifice area

In addition, for $\bar{x} > 4$

$$M_{fs} = 1.23\ \delta^{0.4}\ Kn_N^{-0.4} \tag{22a}$$

$$\bar{r}_{fs} = \frac{r_{fs}}{D} = 0.238\ \delta^{0.6}\ Kn_N^{-0.6} \tag{22b}$$

Here Kn_N is the nozzle Knudsen number based on the source orifice diameter and source mean free path and δ is a factor less than one which accounts for the change in a molecular velocity due to a single collision. When $\bar{r}_{fs} < 4$, it has been found that I^* is given to a good approximation by taking $\bar{r}_{fs} = 4$ and M_{fs} by Eq. (22a).

For $\bar{r}_{fs} > \bar{r}_{SK}$,

$$\bar{I}^* = \frac{\bar{r}_{fs}^2}{(\bar{r} + \bar{r}_d)^2}\left\{1 + \exp\left[-\frac{\gamma M_{fs}^3}{2}\ \frac{\bar{r}_{SK}\left(\frac{\bar{r}_d + \bar{r}_s}{\bar{r}_d}\right)^2}{\bar{r}_{fs}^2 - \frac{\bar{D}_d^2}{4}\left(\frac{\bar{r}_d + \bar{r}_s}{\bar{r}_d}\right)^2}\right]\right\} \tag{23}$$

if

$$\bar{r}_{fs}^2 < Dd^2\,(\bar{r}_d + \bar{r}_s)^2/4\,\bar{r}_d^2$$

the exponential term is taken as zero. Here M_{fs} and $\bar{r}_{fs}$ are given by Eq. (22).

Depending on the geometry of the test apparatus, either Eq. (21) or Eq. (23) will provide the basis from which to measure the scattering loss. The total reduction in the beam is taken to be

$$\frac{I}{I_o} \equiv \left(\frac{I}{I_o}\Big|_w\right)\left(\frac{I}{I_o}\Big|_b\right)\left(\frac{I^*}{I_o}\right)$$

or

$$I = I^*\left(\frac{I}{I_o}\Big|_w\right)\left(\frac{I}{I_o}\Big|_b\right) \qquad (24)$$

where $(I/I_o|_w)$ is the loss of jet particles due to reflected molecules from the chamber wall, $(I/I_o|_b)$ is the loss of jet particles due to the residual background, and I^* represents the effect of the detector geometry.

A comparison of Eq. (24) with the data of several investigators will be made in the next section.

SECTION III
COMPARISON WITH EXPERIMENT

3.1 Evaluation of Constants

Equations (19) and (24) were evaluated for data of several investigators. The values of the σ_{Bj} and σ_{bj} were taken from Ref. 12 for viscous collision cross sections. In addition, $\bar{\sigma}_{jB} = 2\bar{\sigma}_{Bj}$ and $\bar{\sigma}_{jb} = 2\bar{\sigma}_{bj}$ were used for the jet-background interactions to account for the fact that even "glancing collisions" with background molecules can alter the trajectory of a jet particle sufficiently that it will not reach the detector. The geometries of the test apparatus were obtained from Refs. 3, 13, and 14 for Fenn and Anderson data; from Ref. 6 for Govers data; and from personal communication with Messrs. Brown, Heald, Busby, and Ruby for the corresponding data. The value of δ was somewhat arbitrarily taken to be 0.2 (subsequent calculations with $\delta = 0.1$ and 0.3 show no significant difference).

3.2 PREDICTION OF THE FENN AND ANDERSON PARAMETER

The data of several investigators have been collected by Fenn and Anderson in Ref. 3. A comparison of the predicted values as given by a numerical solution of Eq. (19) and these data are shown in Fig. 6. While a slight amount of scatter is observed, in general, the data are matched quite well. Figure 6 also compares the data of Govers et al (Ref. 6) with Eq. (19). The same generally good agreement is also observed.

However, the background pressure effects observed by Brown and Heald (Ref. 4) are not adequately predicted by the theory. This is a result of the definition of $\bar{P}_{b_\infty}$ employed by these investigators. The recorded values of background pressure were measured within the jet plume. Therefore, the assumption of a random $\bar{P}_{b_\infty}$ is not satisfied, and hence, close agreement should not be expected.

3.3 PREDICTION OF TOTAL INTENSITY

A comparison of Eq. (24) with the data of Fenn and Anderson (Ref. 3) for measurements of total intensity versus nozzle-skimmer separation distance is made in Fig. 7. The data are predicted quite well for the range of source diameters, source pressures, and background pressures given. The deviation observed near the data maxima results from the inability of the model to predict transition and continuum effects.

The results of a comprehensive investigation of background effects were presented by Govers, et al, in Ref. 6, where intensities at various values of $\bar{P}_{b_\infty}$ and $\bar{\tau}$ were obtained. A comparison of theory with representative data from this reference is illustrated in Fig. 8. The overall agreement is quite good. At larger values of background pressure and nozzle skimmer separation distance, an increasing mismatch is observed. Since the Mach disc tends to move upstream with increasing source pressure to background pressure ratio and since the Mach disc is expected to occur in the vicinity of the region under investigation for the higher values of $\bar{P}_{b_\infty}$, it is reasonable to expect that some of this mismatch is attributable to the onset of viscous effects in the vicinity of the skimmer.

The prediction of total intensity as a function of source pressure for various source conditions is illustrated in Figs. 9, 10, and 11. The solid curves are calculated for $\bar{P}_{b_\infty} = 0$. Corrections have been made for magnitude of residual background pressure using Eq. (18) where this information was available. The trends displayed by the data are well matched for the lower source pressures; however, at the higher pressures, a deviation from the data is evidenced. Correction for $\bar{P}_{b_\infty}$ remedies this situation for the Brown and Heald data (Fig. 9). (Note: For these data, $\bar{P}_{b_\infty}$ was not measured within the jet expansion.)

The continued discrepancy observed in Fig. 10 and in the warm skimmer of Fig. 11 may be attributed to the pumping system. The end wall of the test chamber is cryogenically pumping, in addition to the side walls as described in Ref. 4. The principle of cryogenic pumping is to remove gases from the chamber by "freezing" them on contact. Therefore, with extensive cryogenic pumping, it is reasonable to expect that only a few molecules will have multiple collisions with the chamber walls. This means that a randomly distributed background will not exist throughout the chamber and gage readings would be strongly dependent on location.

An interesting point is brought to light by Fig. 12 which is a replot of Fig. 11 with higher mass numbers included. When the wall effects have been removed as for the case of the cryogenic skimmer, there is no dip in the intensity curve, and the theory predicts the data quite well. If the onset of condensation is connected in some way with this dip as is hypothesized in Refs. 15 and 16, the intensity of higher mass numbers should also decrease. As seen in the figure, the relative peaks are higher although shifted slightly. In fact, it appears that reduction of the wall effects tends to increase the intensity and remove the dip, whereas the higher mass numbers peak at approximately the same place. Therefore, it appears that the dip is much more closely connected with scattering effects than with the onset of condensation.

The unpublished results of a current investigation by Benek and Busby to verify the above hypothesis are shown in Figs. 13, 14, 15, and 16. These data were obtained for the skimmer-wall configurations shown in Fig. 17. The background pressure was measured at a point approximately midway between the source and skimmer by an ion gage which was shielded from the jet (Fig. 17). It was hoped that this procedure would yield the average pressure in the region surrounding the jet.

The theory is seen to accurately predict these data. Since the theoretical values for zero background pressure are the same as those given in Fig. 11, the only difference between the corresponding warm skimmer and cold donut data is the magnitude of background pressure. The mismatch observed in Figs. 13 and 14 at $P_o > 700$ torr is attributed to the onset of continuum and transition effects. The discrepancy in Figs. 15 and 16 beginning at approximately $P_o > 900$ to 1000 torr is attributed to high collimation section pressures (hence beam scattering). In fact, the collimation pressures for these deviations are within 11 to 30 percent of each other depending on the points taken for "signification deviation." The "dip" observed in the intensity-source pressure curve is reasonably well predicted by considering only the scattering phenomenon. Since the dip is generally associated with condensation effects, there may be a closer connection between these two phenomena than has previouly been suspected.

SECTION IV
COMPARISON WITH PREVIOUS THEORY

As noted earlier an informative model of the scattering process has been proposed by Muntz et al (Ref. 8). The expression obtained for the correlation parameter, Eq. (1), including all corrections for a finite test volume is

$$-\frac{\partial}{\partial \bar{P}_{b_\infty}}\left(\ell n\ \frac{I}{I_o}\right) = \frac{\bar{\nu}'\pi\,\bar{\sigma}_{JB}^{\,2}\,\bar{r}_p}{\bar{T}_{b_\infty}}\ e^{\bar{r}_p/\bar{r}_c\int_{\bar{r}^*}^{\bar{r}}\exp\left(-\frac{\bar{r}_p}{\bar{x}}\right)d\bar{x}} \tag{25}$$

where

$$\bar{r}_p \equiv \frac{\zeta\,\pi\,\bar{\nu}'\bar{\sigma}_{BJ}^{\,2}\,\eta\,\bar{r}^{*2}}{\bar{C}_B'},\quad \bar{\nu}' = \left(\frac{V_j + C_B'}{V_j}\right)$$

and

$$0 \le \zeta \le 1$$

and accounts for uncertainty in the number of collisions to effectively stop a background particle. The effects of the wall are included in $\bar{r}_c$ which is taken to be the distance from the source at which the background-background particle collision frequency is equal to the background jet particle collision frequency. This term was given to be

$$\bar{r}_c^{\,2} = \frac{\bar{\nu}'\bar{\sigma}_{BJ}^{\,2}\,\bar{r}^{*2}}{\bar{\bar{C}}_B'\,\bar{\sigma}_{BB}^{\,2}\,\bar{n}_{b_\infty}}$$

where

$$\bar{\bar{C}}_B' = A\,\bar{C}_B,\ 0 \le A \le 1$$

and $\bar{C}_B$ is the mean background particle velocity based on the effective wall temperature and $\bar{\sigma}_{BB}$ is the background-background collison cross section.

However, at this point it should be noted that Eq. (25) is not correct. The error results from neglecting the dependence of $\bar{r}_c$ on $\bar{P}_{b_\infty}$ in the differentiation to obtain Eq. (23). The expression including this dependence is

$$\frac{\partial}{\partial \bar{P}_{b_\infty}}\left(\ell n \frac{1}{I_o}\right) = -\frac{\bar{\nu}' \pi \bar{\sigma}_{B_j}^2 \bar{r}_p}{\bar{T}_{b_\infty}} e^{\bar{r}_p/\bar{r}_c}\left[1 + \frac{1}{2}\frac{\bar{r}_p}{r_c}\right]\int_{\bar{r}^*}^{\bar{r}} \exp\left(-\frac{\bar{r}_p}{\bar{x}}\right) d\bar{x} \qquad (26)$$

It can readily be seen that both Eqs. (25) and (26) have an intrinsic dependence on the magnitude of background pressure which is absent in the experimental data. Such a dependence should lead to poor agreement with the experimental data. In addition, it is to be expected that Eq. (26) will deviate more rapidly.

Both of these equations have been evaluated for sample data of Ref. 3, for two values of background pressure. The agreement with the data is illustrated in Fig. 18. As expected Eq. (26) deviates more rapidly. However, it must be noted that the trends shown by the experimental evidence are followed. The present theory matches the data while avoiding the difficulties of dependence on magnitude of background pressure.

SECTION V
CONCLUSIONS AND RECOMMENDATIONS

The comparison in the previous section of the predicted values of the Fenn and Anderson parameter and intensity as a function of either separation distance or source pressure with the data tends to confirm the validity of the proposed theory. Two important aspects of measurements made from free-jet expansions have been placed in perspective. First, the background consists of two separable components: (1) the jet particles reflected from the chamber walls, and (2) the residual unpumped gases in the chamber. Second, the dip in intensity versus source pressure curve can be closely associated with molecular scattering.

It is recommended that future condensation studies be conducted with scattering effects in mind. In particular, the connection between these two phenomena at the "dip" should be given careful consideration since they both seem to become dominate in this region.

REFERENCES

1. Benek, J. A. and Powell, H. M. "An Investigation of Performance Parameters of a Mass Spectrometer Sampling Probe in Rarefied Flows." AEDC-TR-70-79 (AD707843), June 1970.

2. Ashkenas, H. and Sherman, F. S. "The Structure and Utilization of Supersonic Free Jets in Low Density Wind Tunnels." Fourth International Symposium on Rarefied Gas Dynamics, Vol. 2, J. H. de Leeuw, editor, Academic Press, Inc., New York, 1965, pp. 84-105.

3. Fenn, J. B. and Anderson, J. B. "Background and Sampling Effects in Free Jet Studies by Molecular Beam Measurements." Fourth International Symposium on Rarefied Gas Dynamics, Vol. 2, J. H. de Leeuw, editor, Academic Press, Inc., New York, 1965, pp. 311-330.

4. Brown, R. F. and Heald, J. H., Jr. "Background and Skimmer Interaction Studies Using a Cryogenically Pumped Molecular Beam Generator." Proceedings of Fifth International Symposium on Rarefied Gas Dynamics, C. L. Brundin, editor, Academic Press, Inc., New York, 1967, pp. 1407-1424.

5. Bossel, Ulf. "Investigation of Skimmer Influences on the Production of Aerodynamically Intensified Molecular Beams." College of Engineering Report No. AS-68-6, University of California, Berkeley, California, August 1968.

6. Govers, T. R., LeRoy, R. L., and Deckers, J. M. "The Concurrent Effects of Skimmer Interaction and Background Scattering on the Intensity of a Supersonic Molecular Beam." Sixth International Symposium on Rarefied Gas Dynamics, Vol. 2, L. Trilling and H. Y. Wachman, editors, Academic Press, Inc., New York, 1969.

7. Ruby, E. C., Brown, R. F., and Busby, M. R. "The Effects of Condensation in the Flow Field Properties in Free-Jet Expansion of Argon." AEDC-TR-70-142 (AD710616), August 1970.

8. Muntz, E. P., Hamel, B. B., and Maguire, B. L. "Exhaust Plume Rarefaction." AIAA Paper No. 69-557, AIAA Fluid and Plasma Dynamics Conference, San Francisco, California, June 1969.

9. Shaw, L. M. and Hickman, R. S. "Comparison of Predicted and Measured Low Density Plume Impingement Effects." Journal of Spacecraft and Rockets, Vol. 6, No. 11, November 1969.

10. Wilmoth, R. G. and Hagena, O. F. "Scattering of Argon and Nitrogen off Polycrystalline Nickel." University of Virginia Report No. AEEP-4038-105-67U, Charlottesville, Virginia, August 1967.

11. French, J. B. "Continuum-Source Molecular Beams." AIAA Journal, Vol. 3. June 1965, pp. 993-1000.

12. Hirschfelder, J. O., Curtiss, C. F. and Bird, R. B. Molecular Theory of Gases and Liquids. John Wiley & Sons, Inc., New York, 1954.

13. Anderson, J. B. and Fenn, J. B. "Velocity Distributions in Molecular Beams from Nozzle Sources." The Physics of Fluids, Vol. 8, May 1965, pp. 780-787.

14. Deckers, J. and Fenn, J. B. "High Intensity Molecular Beam Apparatus." The Review of Scientific Instruments, Vol. 34, January 1963, pp. 96-100.

15. Hagena, O. F. and Morton, H. S., Jr. "Analysis of Intensity and Speed Distribution of a Molecular Beam from a Nozzle Source." Fifth International Symposium on Rarefied Gas Dynamics, Vol. 2, C. L. Brundin, editor, Academic Press, Inc., New York, 1967, p. 1376.

16. Golomb, D., Good, R. E., and Brown, R. F. "Dimers and Clusters in Free Jets of Argon and Nitric Oxide." Journal of Chemical Physics, Vol. 52, February 1970, pp. 1545-1551.

APPENDIXES

I. ILLUSTRATIONS

II. EVALUATION OF THE SCATTERING INTEGRAL

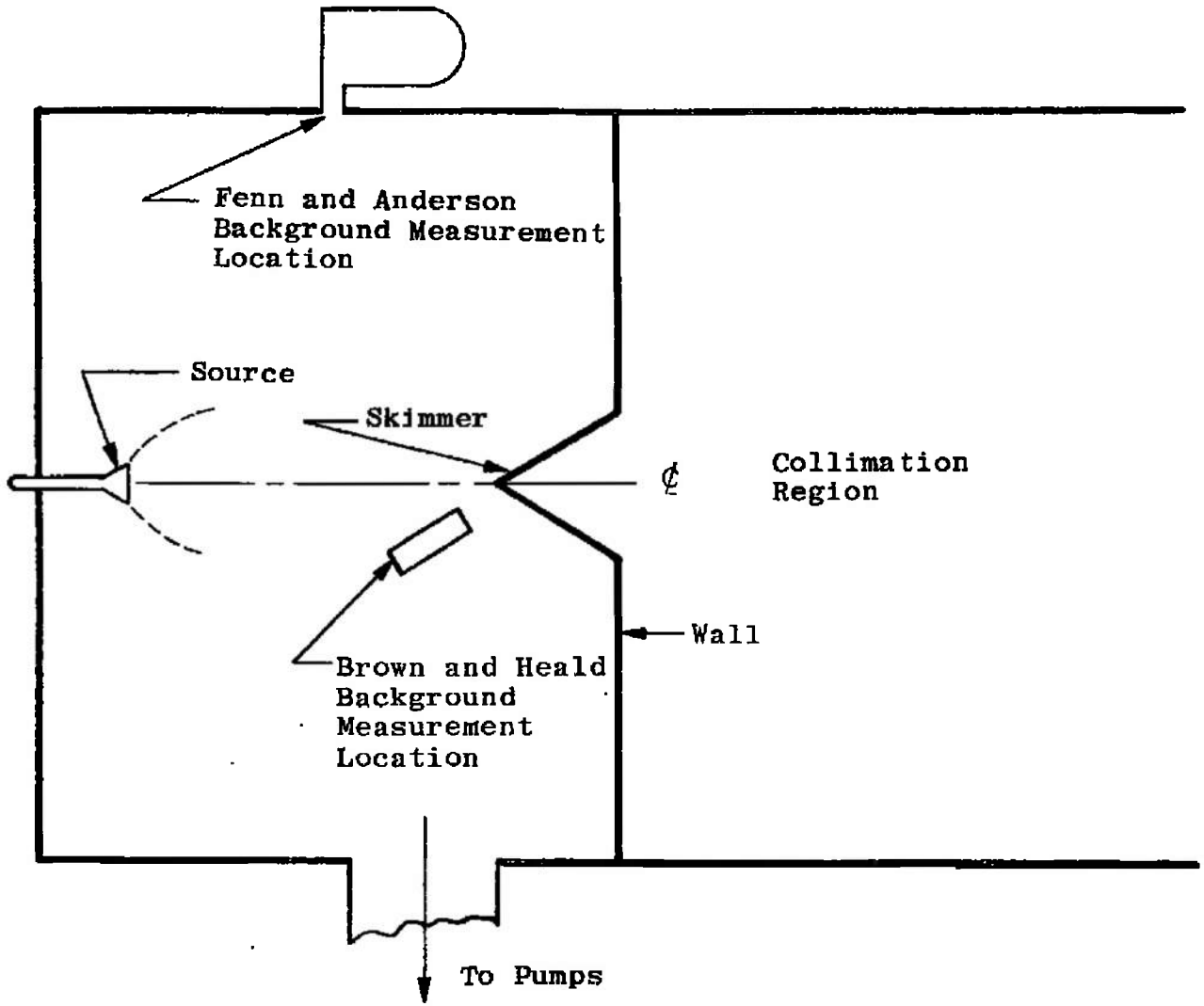

Fig. 1 Typical Molecular Beam Apparatus

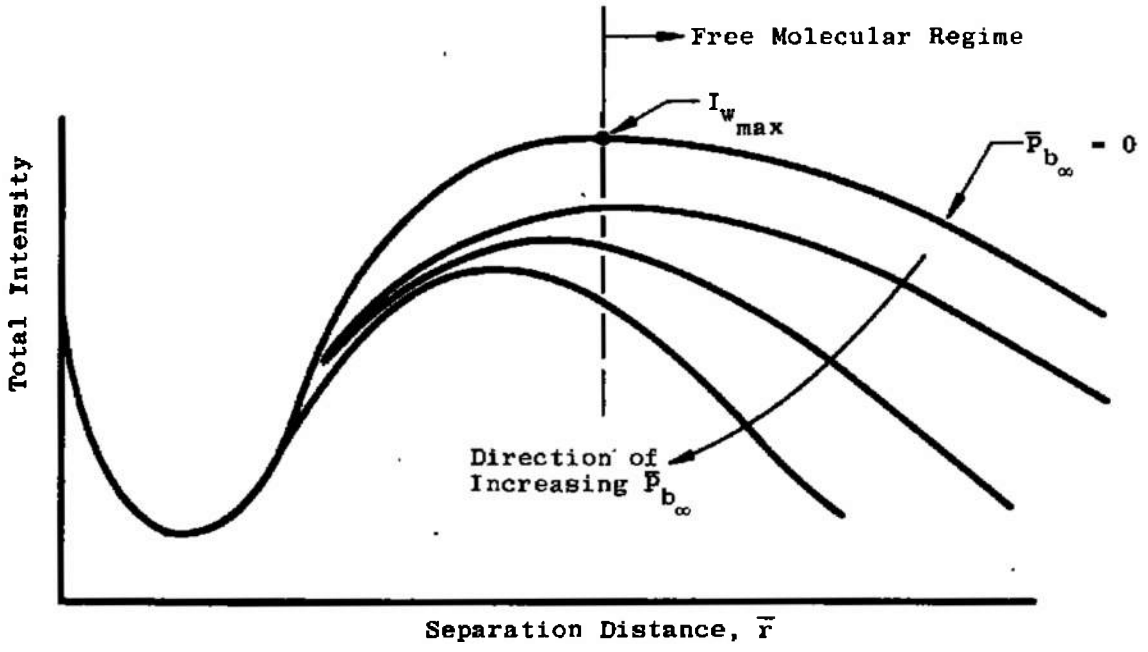

a. Variation of Total Intensity with Separation Distance and Background Pressure

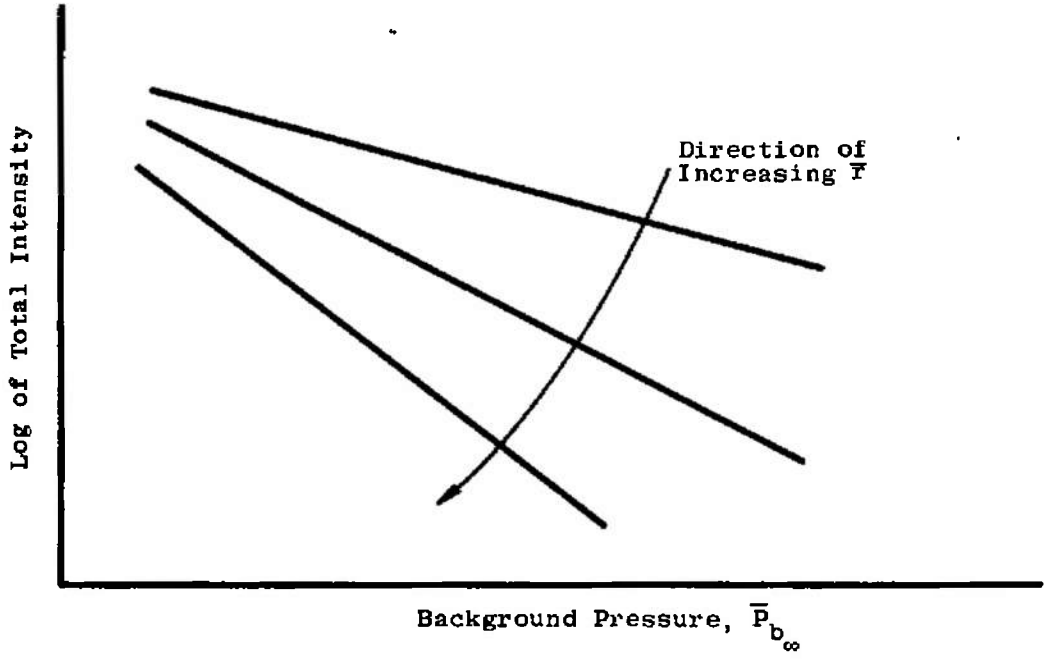

b. Semilog Cross Plot of Fig. 2a Showing Linear Dependence of Total Intensity on Background Pressure for Several Values of Separation Distance

Fig. 2 Typical Background Pressure Data Dependence

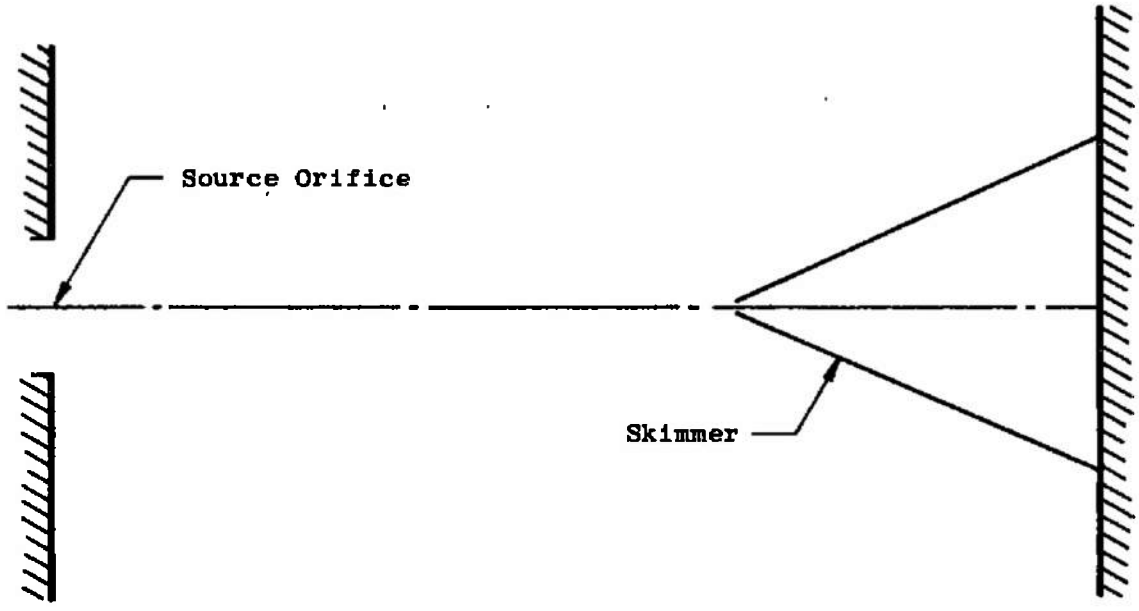

a. Actual Configuration

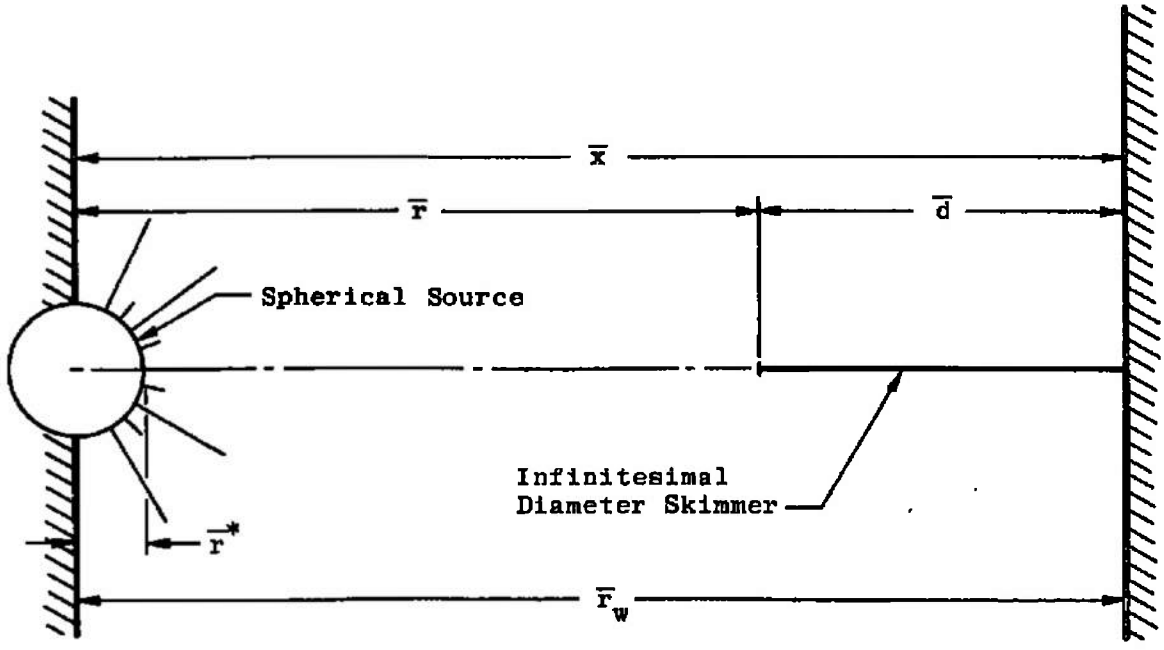

b. Mathematical Model of Fig. 3a

Fig. 3 Coordinate System

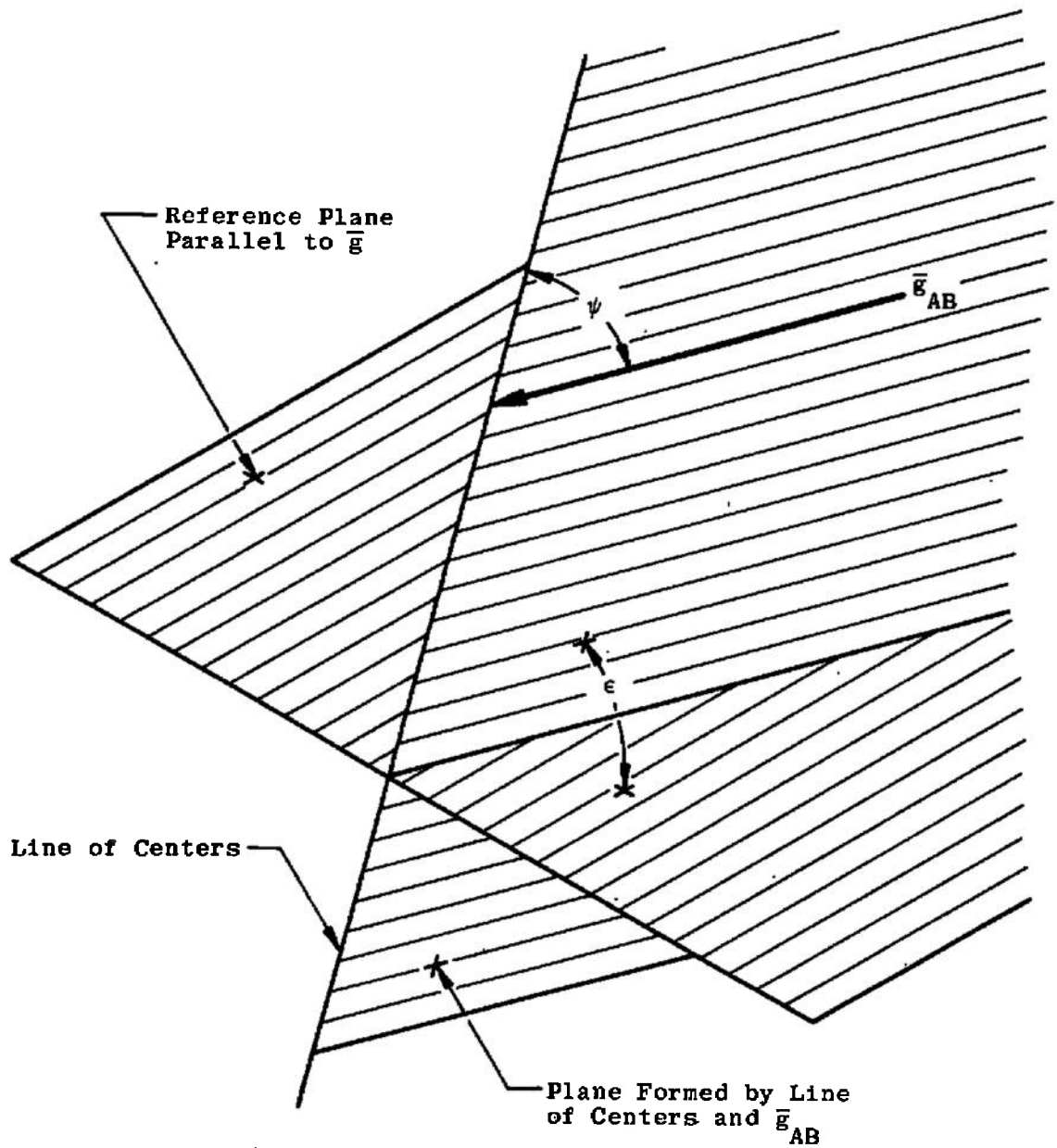

Fig. 4 Definition of the Collision Parameters ϵ and ψ

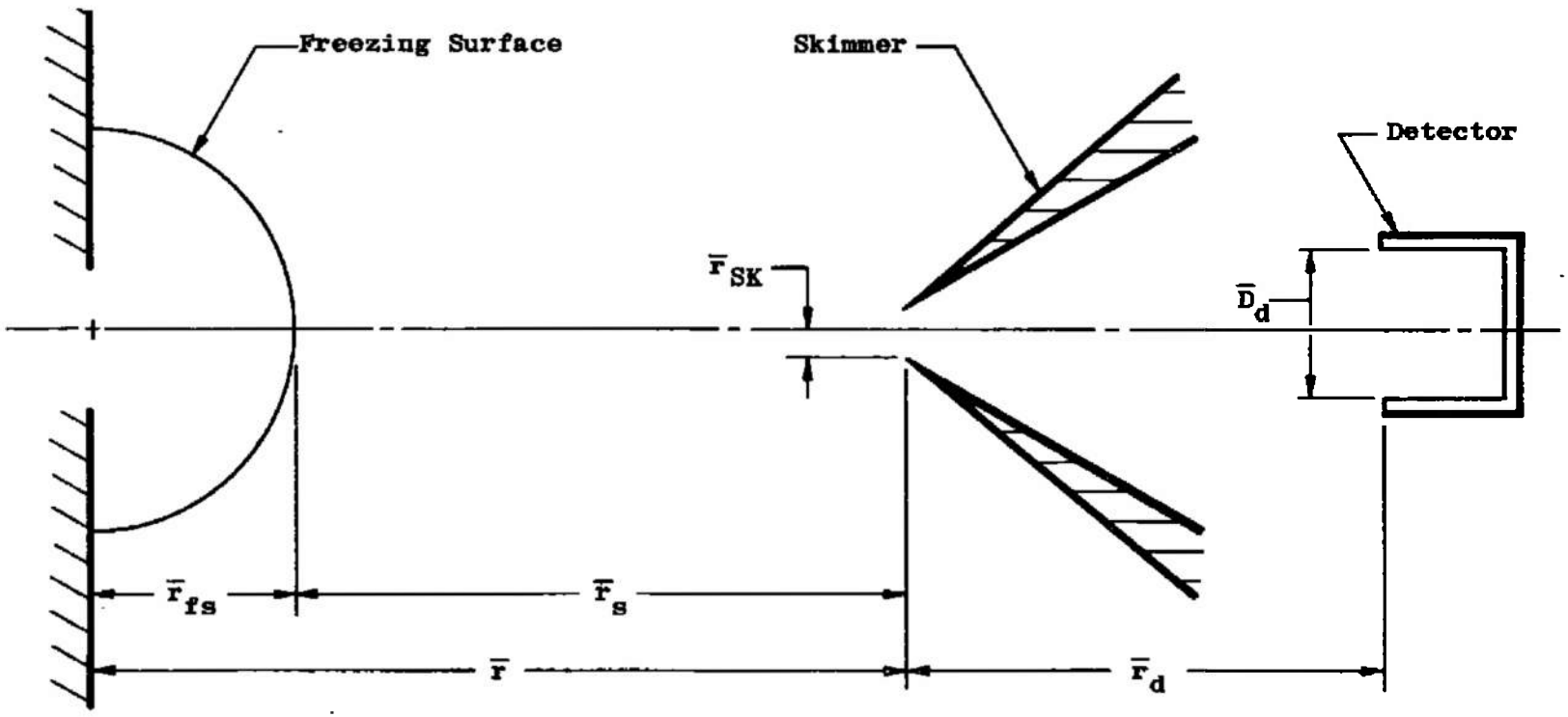

Fig. 5 Geometry for Fenn's Intensity Correction

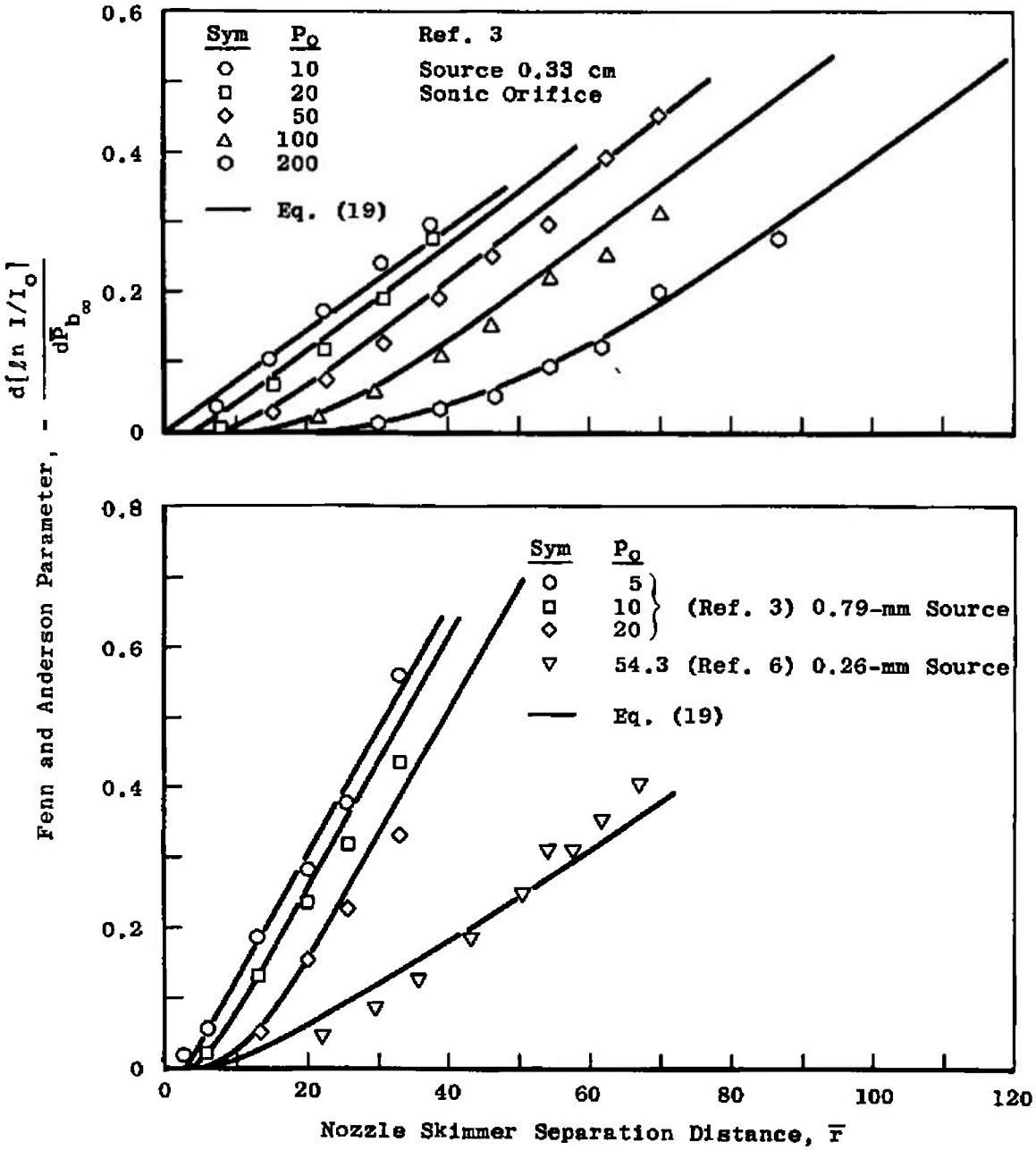

Fig. 6 Prediction of the Fenn and Anderson Parameter

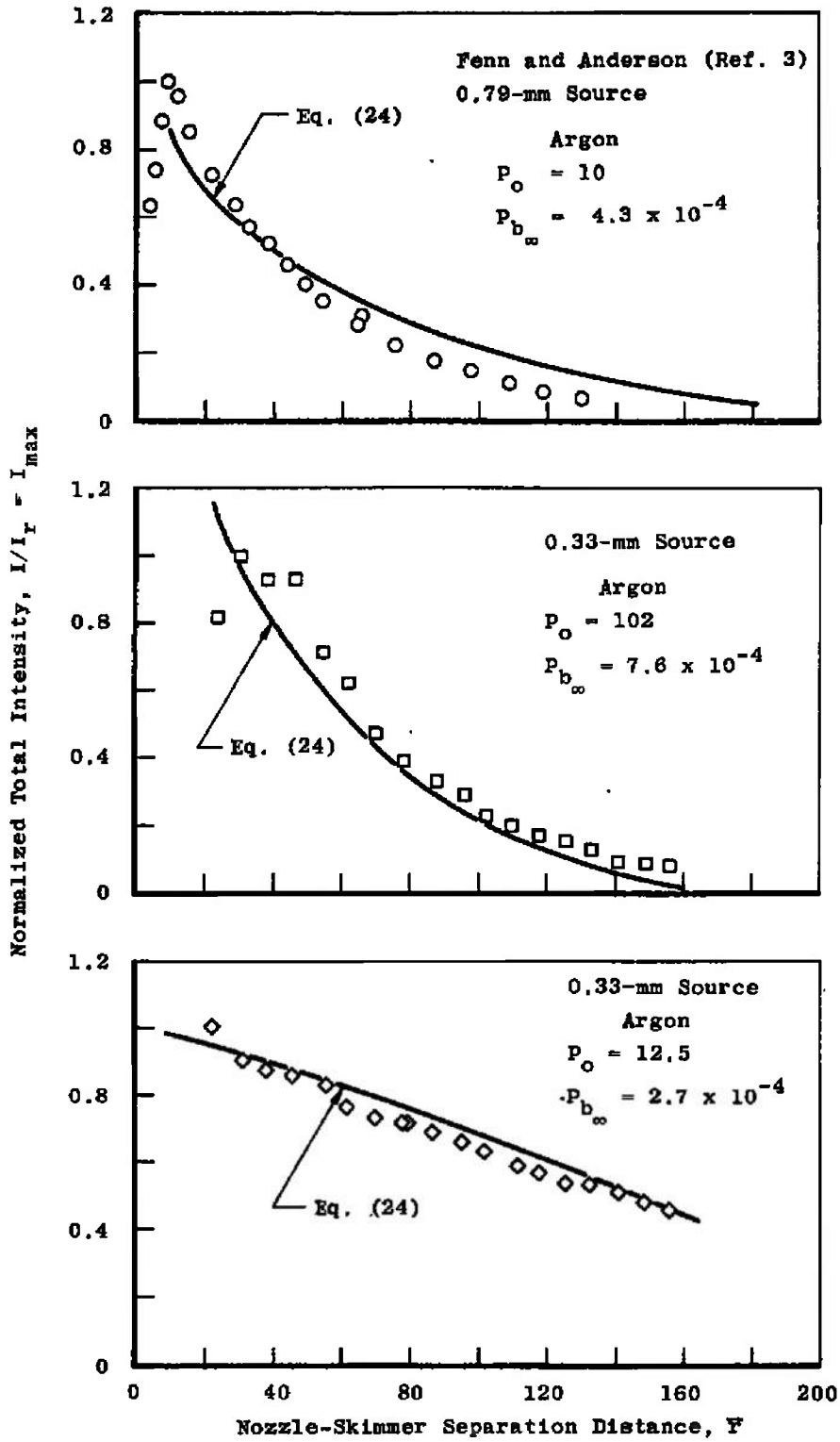

Fig. 7 Comparison of Theory with Fenn and Anderson Total Intensity versus Separation Distance Data

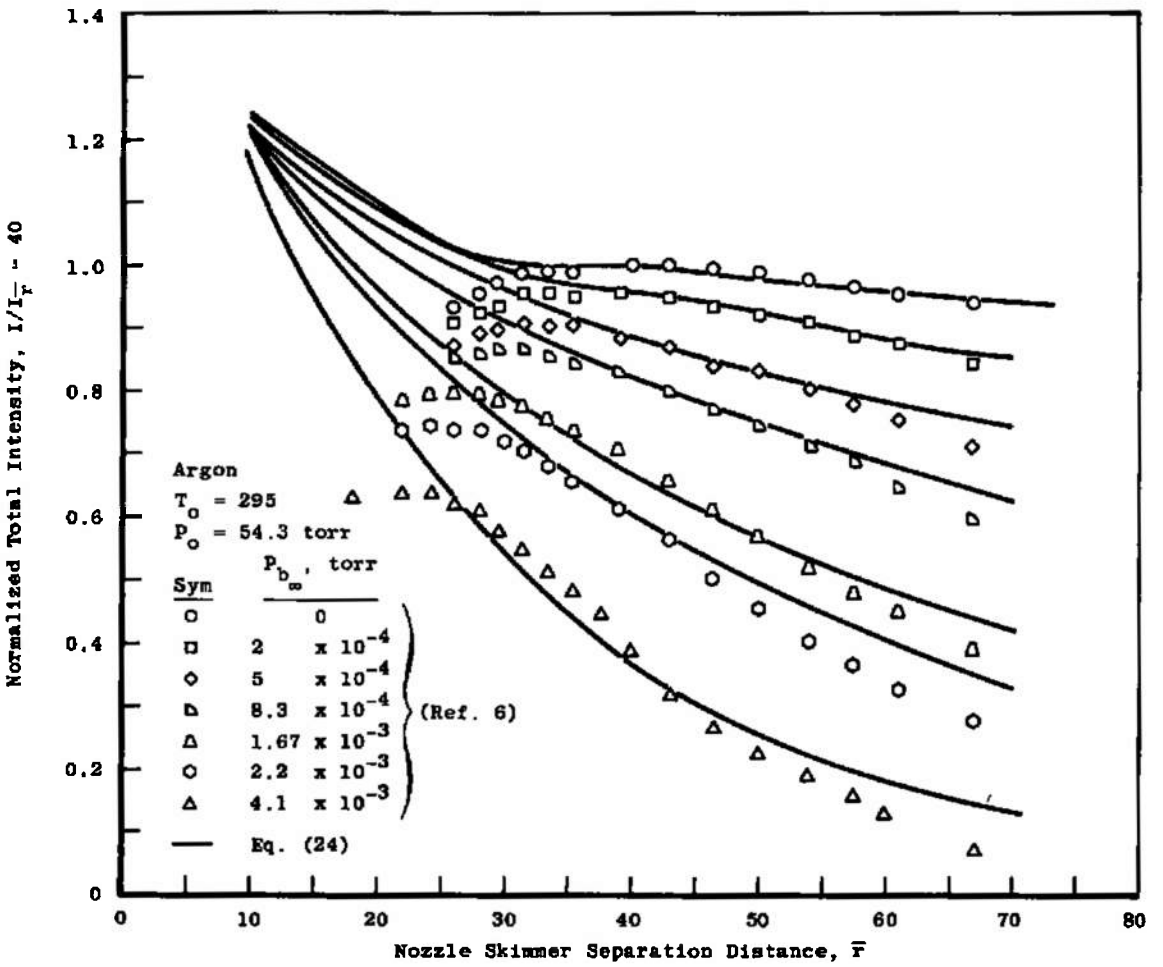

Fig. 8 Comparison of Theory with Gover et al Total Intensity versus Separation Distance Data

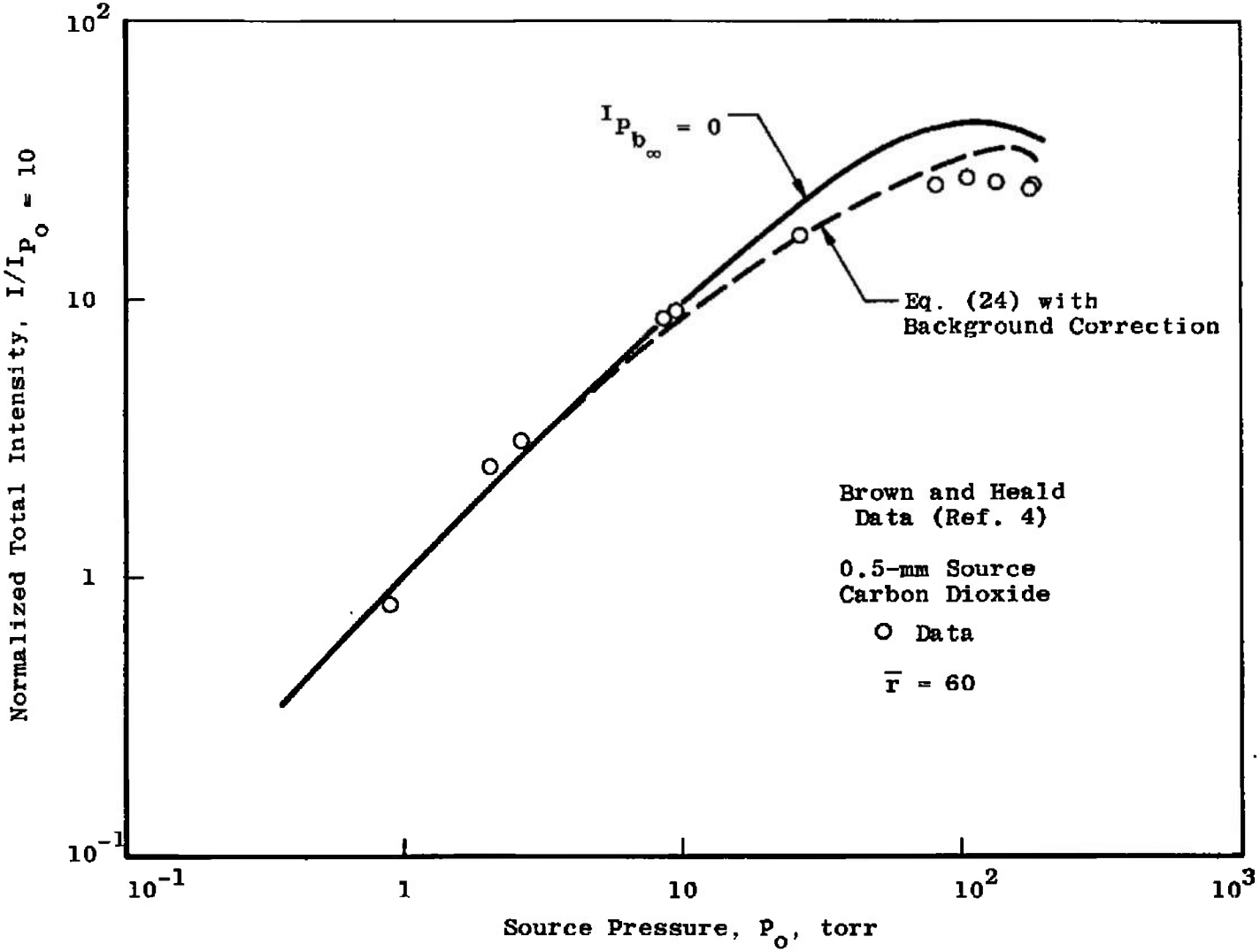

Fig. 9 Prediction of Brown and Heald Total Intensity versus Source Pressure Data

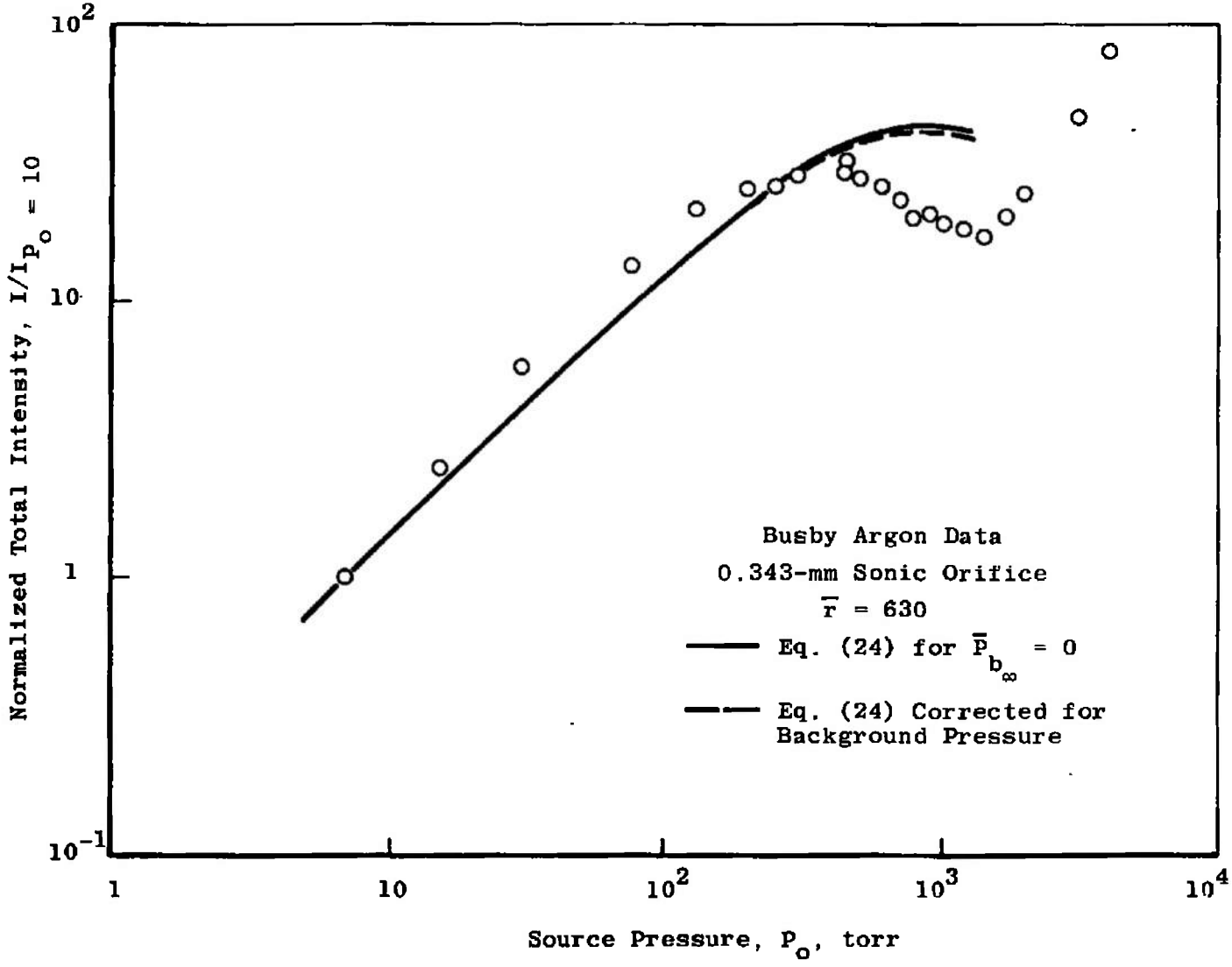

Fig. 10 Prediction of Unpublished Total Intensity versus Source Pressure Data of Busby

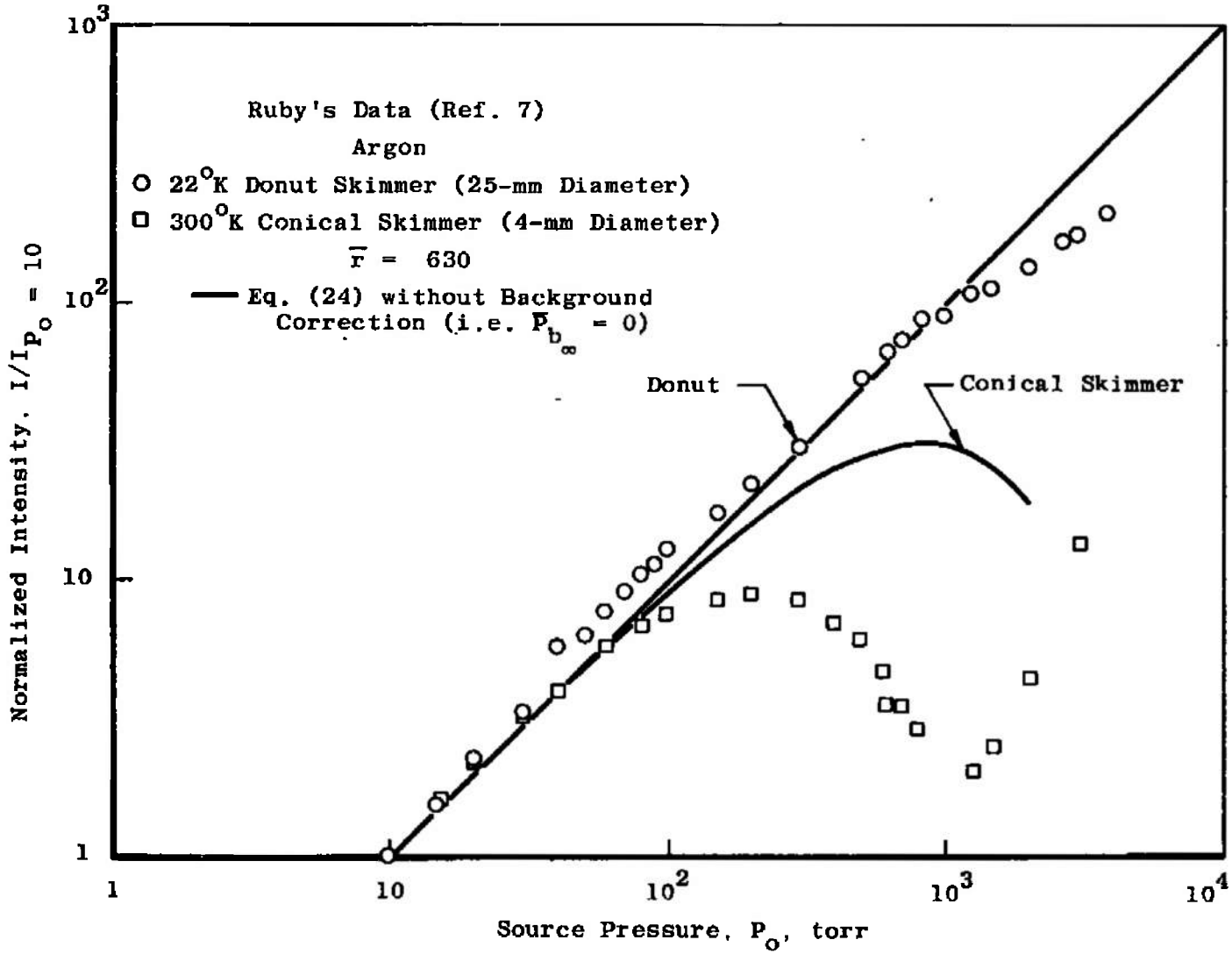

Fig. 11 Prediction of Ruby's Total Intensity versus Source Pressure Data

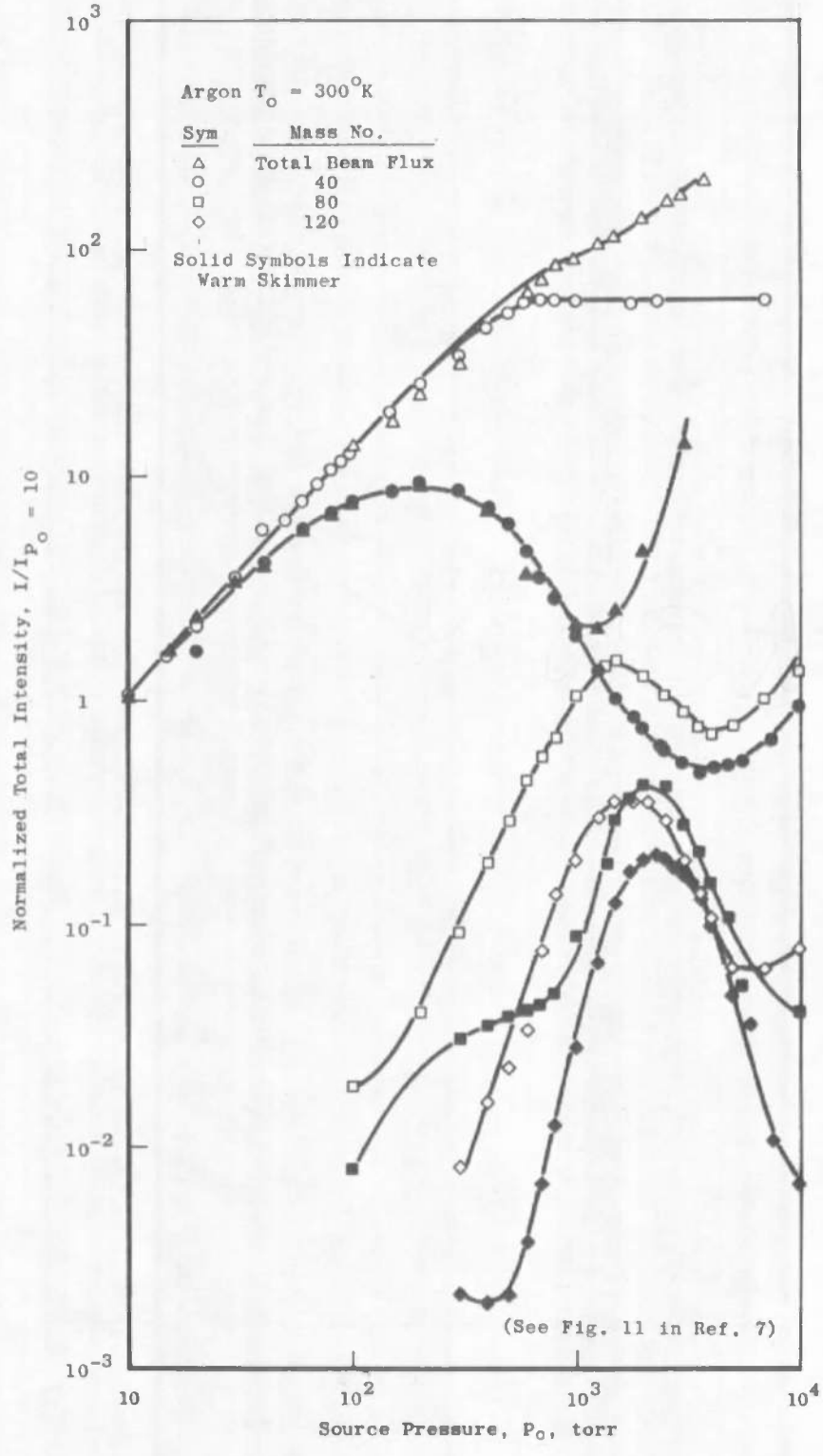

Fig. 12 Condensation Effects for Warm and Cold Donut

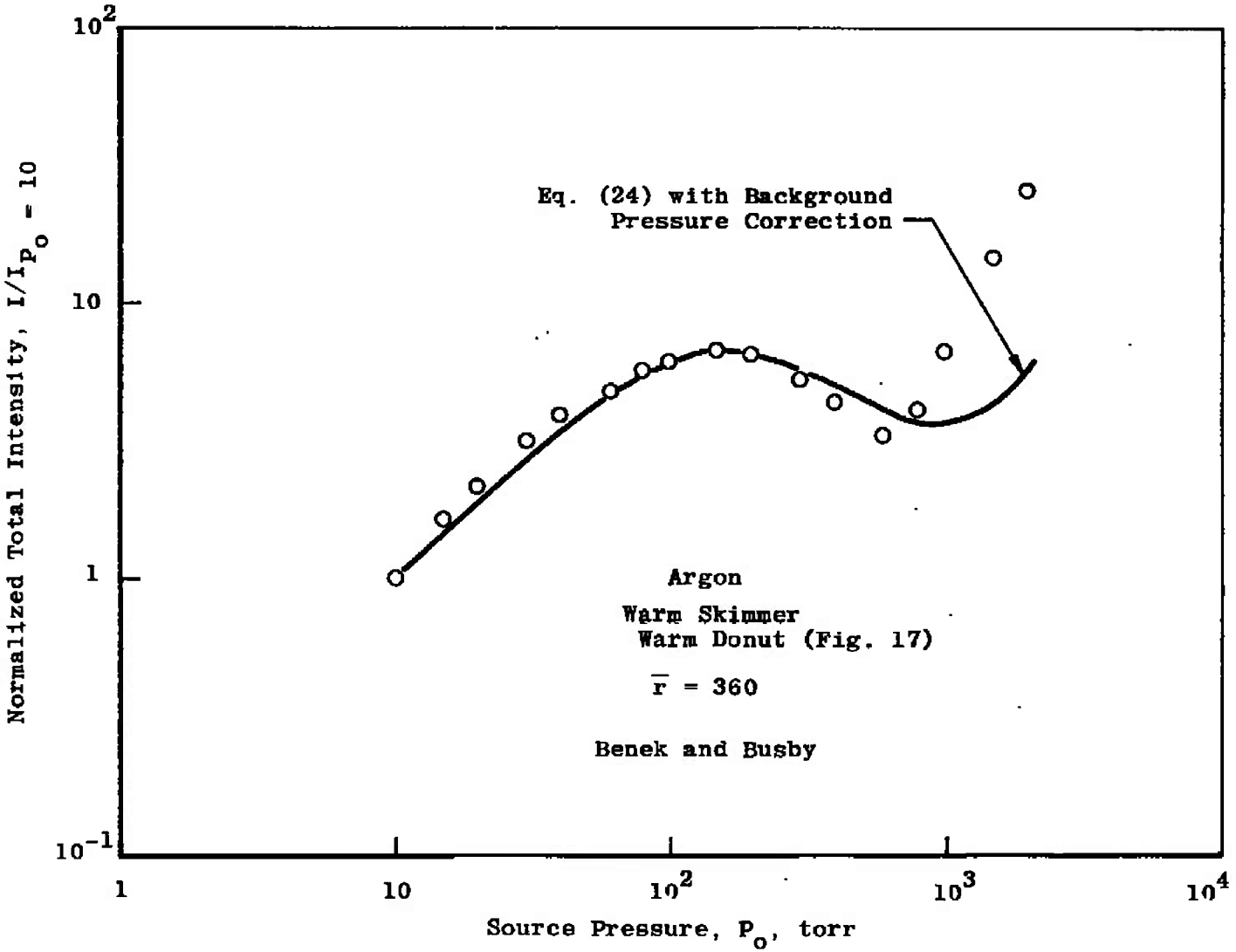

Fig. 13 Comparison of Theory with Warm-Skimmer Warm-Donut Total Intensity versus Source Pressure Data

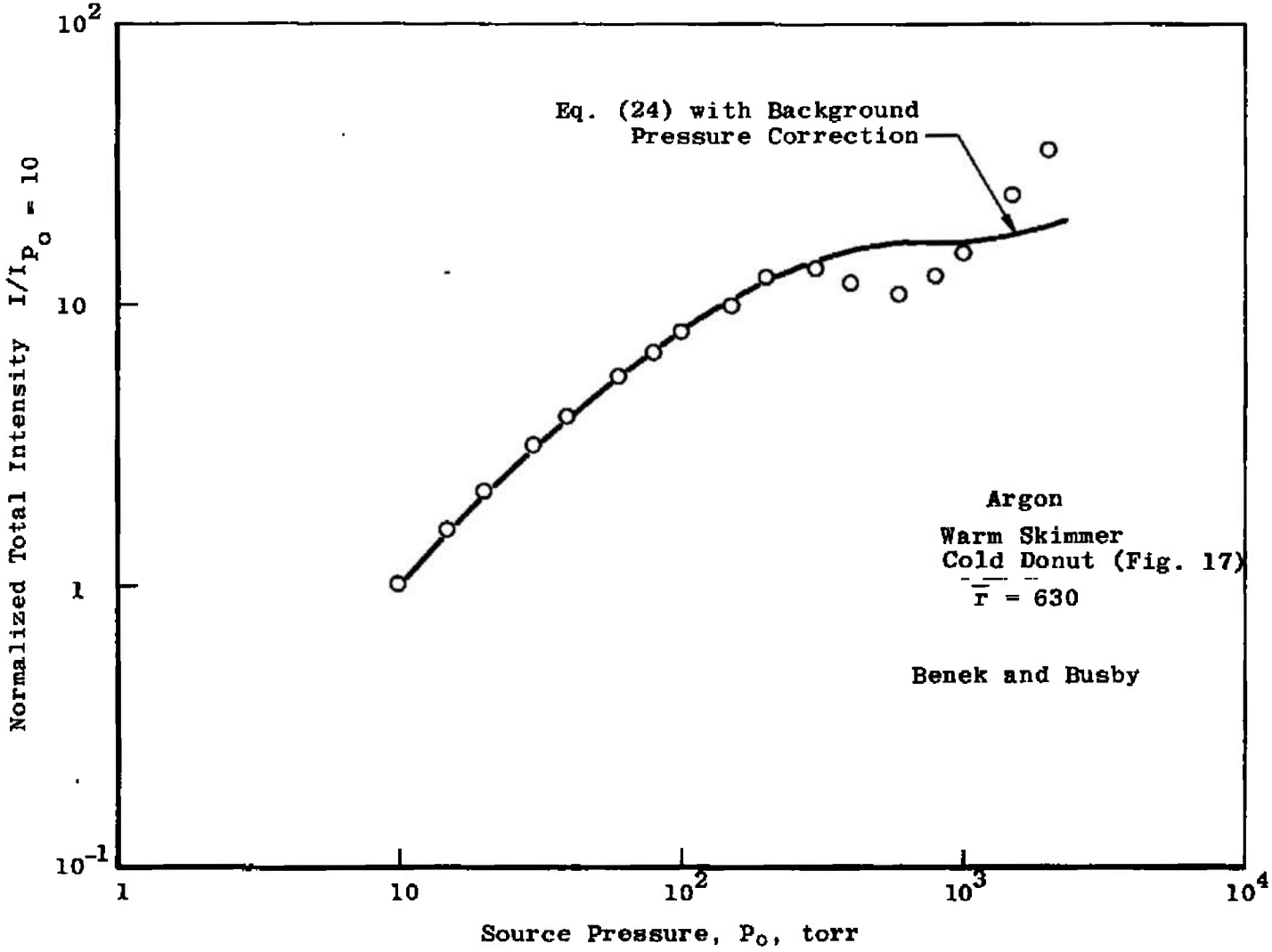

Fig. 14 Comparison of Theory with Warm-Skimmer Cold-Donut Total Intensity versus Source Pressure Data

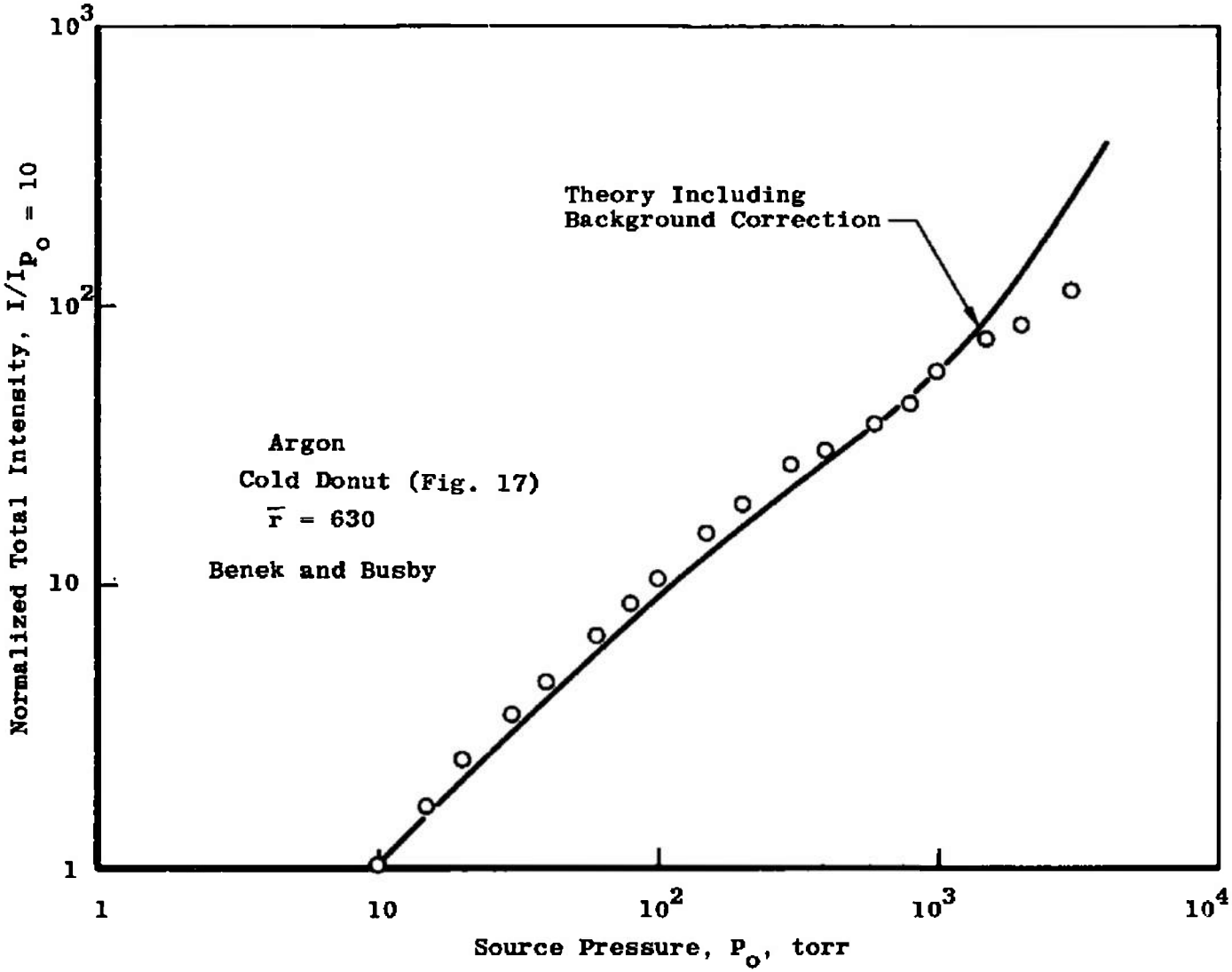

Fig. 15 Comparison of Theory with Cold-Donut Total Intensity versus Source Pressure Data for Argon

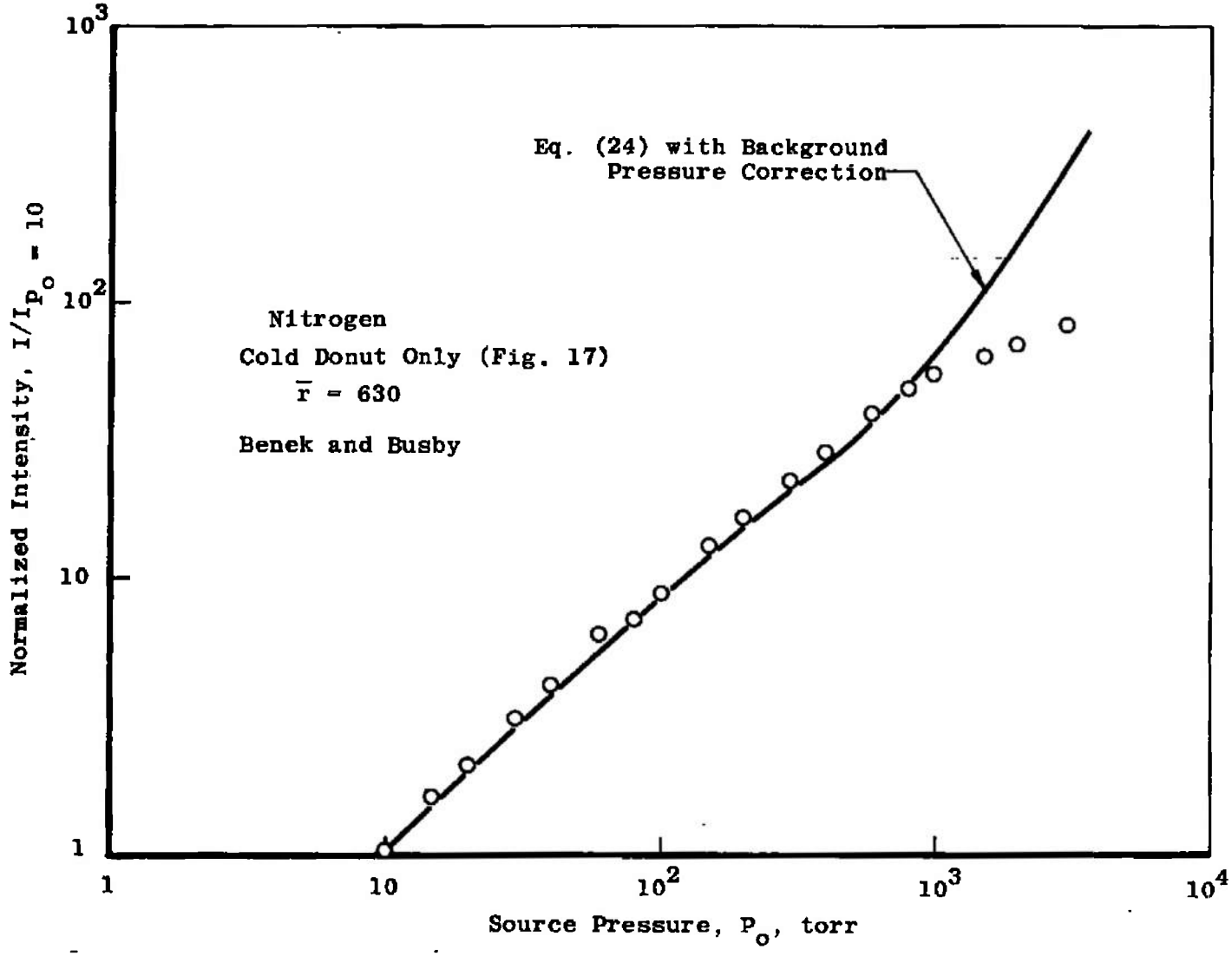

Fig. 16 Comparison of Theory with Cold-Donut Total Intensity versus Source Pressure Data for Nitrogen

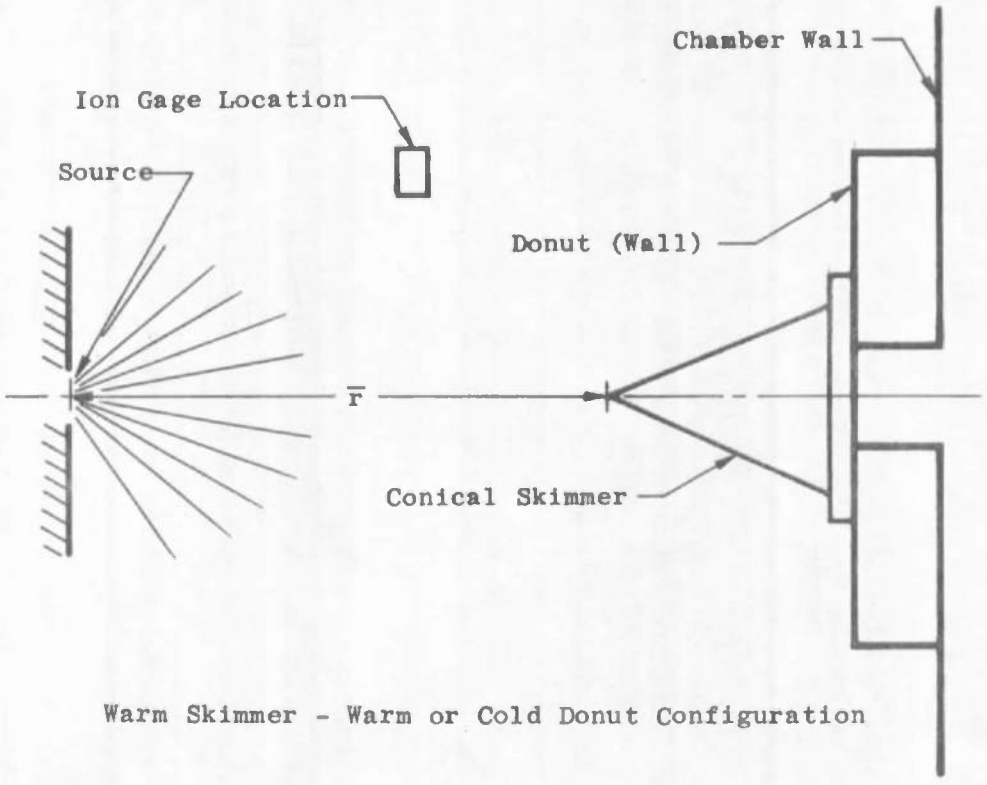

Warm Skimmer - Warm or Cold Donut Configuration

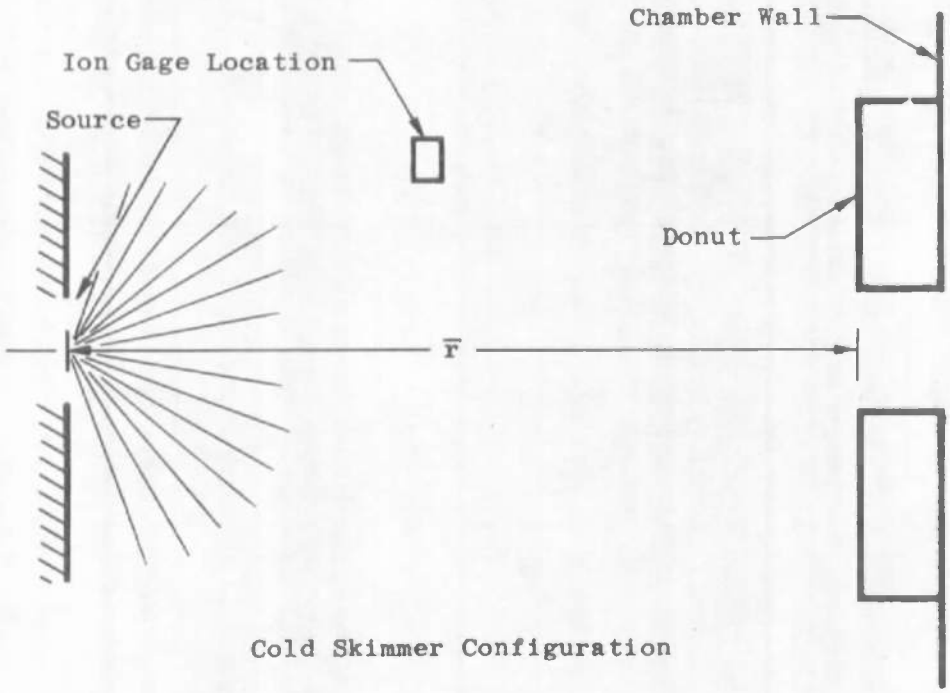

Cold Skimmer Configuration

Fig. 17 Test Configurations

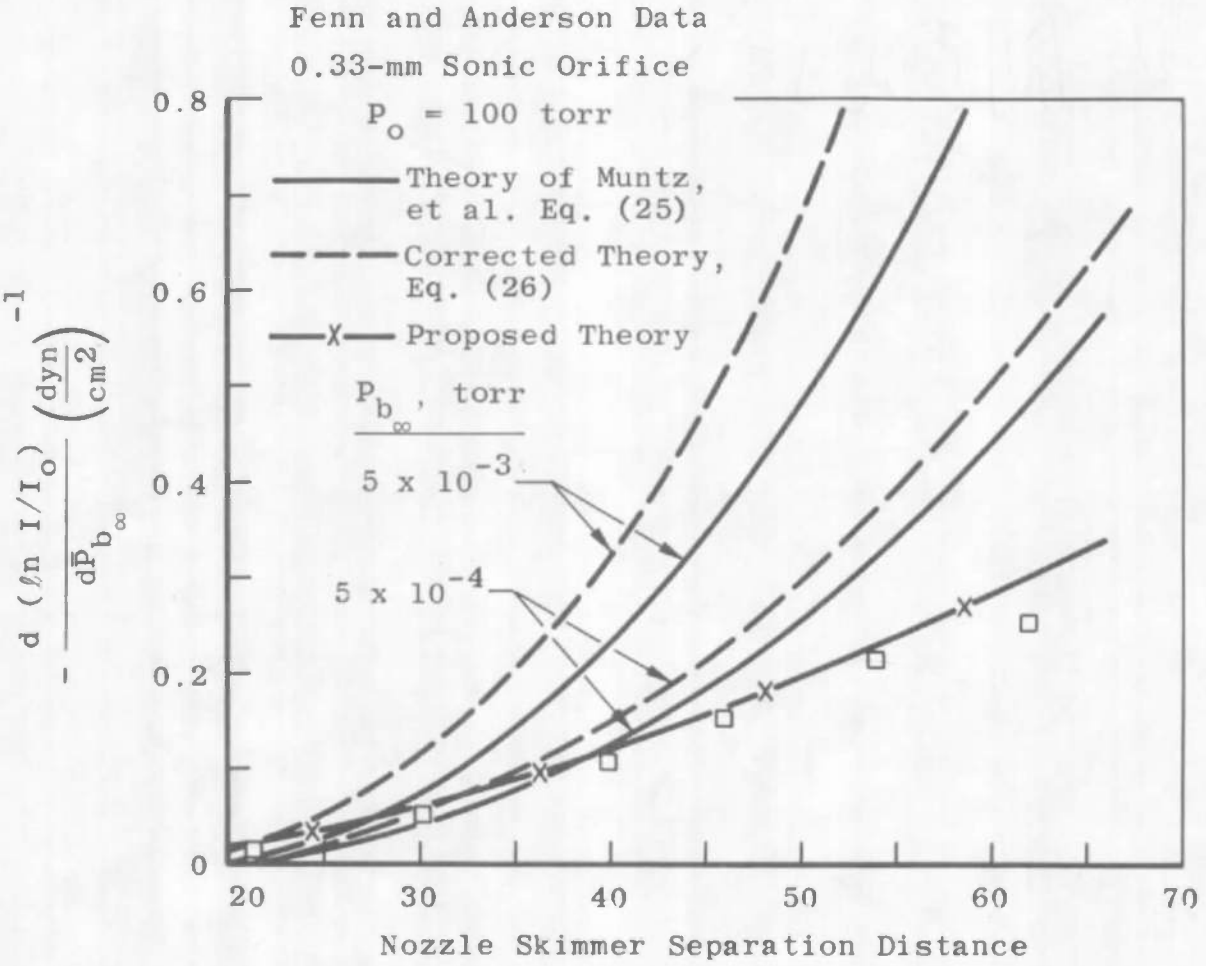

Fig. 18 Illustration of Background Pressure Dependence of Muntz et al Scattering Theory

APPENDIX II
EVALUATION OF THE SCATTERING INTEGRAL

The integral $\int \exp(-\bar{a}/\bar{x})d\bar{x}$ may be integrated once by parts after substituting

$$\xi = \frac{\bar{a}}{\bar{x}}$$

and

$$d\xi = -\frac{\bar{a}}{\bar{x}^2}\,dx$$

where $\bar{a}$ is a constant to obtain

$$\int \frac{\bar{x}^2\, e^{-\xi}}{\bar{a}}\, d\xi = \bar{a} \int \xi^2 e^{-\xi}\, d\xi$$

Integration gives

$$\int \exp\left(-\frac{\bar{a}}{\bar{x}}\right) d\bar{x} = \bar{a}\left[\frac{\bar{x}}{\bar{a}} \exp\left(-\frac{\bar{a}}{\bar{x}}\right) + E_i\left(-\frac{\bar{a}}{\bar{x}}\right)\right]$$

where $E_i(-\bar{a}/\bar{x})$ is the exponential integral and is a known tabulated function.

UNCLASSIFIED

Security Classification

DOCUMENT CONTROL DATA - R & D

(Security classification of title, body of abstract and indexing annotation must be entered when the overall report is classified)

1. ORIGINATING ACTIVITY (Corporate author)	2a. REPORT SECURITY CLASSIFICATION
Arnold Engineering Development Center, ARO, Inc., Operating Contractor, Arnold Air Force Station, Tennessee 37389	UNCLASSIFIED
	2b. GROUP: N/A

3. REPORT TITLE

PREDICTION OF MOLECULAR SCATTERING EFFECTS IN FREE-JET EXPANSIONS

4. DESCRIPTIVE NOTES (Type of report and inclusive dates)

April to May 1970--Final Report

5. AUTHOR(S) (First name, middle initial, last name)

J. A. Benek, ARO, Inc.

6. REPORT DATE	7a. TOTAL NO. OF PAGES	7b. NO. OF REFS
January 1971	47	6

8a. CONTRACT OR GRANT NO.	9a. ORIGINATOR'S REPORT NUMBER(S)
F40600-71-C-0002	
b. PROJECT NO 4344	AEDC-TR-70-273
c. Program Elements 62101F and 65701F	9b. OTHER REPORT NO(S) (Any other numbers that may be assigned this report)
d.	ARO-VKF-TR-70-264

10. DISTRIBUTION STATEMENT

This document has been approved for public release and sale; its distribution is unlimited.

11. SUPPLEMENTARY NOTES	12. SPONSORING MILITARY ACTIVITY
Available in DDC	AEDC, AFSC, Arnold AF Station, Tenn. and AFCRL, L. G. Hanscom Field, Bedford, Mass.

13. ABSTRACT

The effects of background pressure on reduction of molecular beam intensity are investigated. A theoretical model is developed which shows the background to be separable into two distinct components: one attributable to reflected jet particles and the other attributable to residual (unpumped) particles. An expression for the Fenn and Anderson correlation parameter is obtained. Comparisons of the data of several investigators are made with theoretically predicted values of intensity as a function of either separation distance or source pressure. The characteristic dip in the intensity versus source pressure curve has been related to scattering effects as well as to condensation effects.

DD FORM 1 NOV 65 1473

UNCLASSIFIED

Security Classification

14. KEY WORDS	LINK A		LINK B		LINK C	
	ROLE	WT	ROLE	WT	ROLE	WT
free-jet expansion						
molecular flow						
molecular beam						
intensity						
background						
scattering						
separation						
condensation						
mass spectrometer						
sampling						
probes						